RESEARCH ARTICLE

Title: Sulfur oxidation and reduction are coupled to nitrogen fixation in the roots of the salt marsh foundation plant *Spartina alterniflora*

Author list: Rolando, J.L.[1]; Kolton, M.[1,2]; Song, T.[1], Liu, Y.[1,3]; Pinamang, P.[1], Conrad, R.[1]; Morris, J.T.[4], Konstantinidis, K.T.[1,5], Kostka, J.E. [1,6,7]

Affiliations:

[1]Georgia Institute of Technology, School of Biological Sciences, Atlanta, GA 30332, USA

[2]French Associates Institute for Agriculture and Biotechnology of Drylands, Ben-Gurion University of the Negev, Beer Sheva, Israel

[3]The Pennsylvania State University, Department of Civil & Environmental Engineering, University Park, PA, 16802

[4]Belle Baruch Institute for Marine & Coastal Sciences, University of South Carolina, Columbia, SC, 29201

[5]Georgia Institute of Technology, School of Civil and Environmental Engineering, Atlanta, GA 30332, USA

[6]Georgia Institute of Technology, School of Earth and Atmospheric Sciences, Atlanta, GA 30332, USA

[7]Center for Microbial Dynamics and Infection, Georgia Institute of Technology, Atlanta, GA 30332, USA

Corresponding author:

Kostka, JE. e-mail: joel.kostka@biology.gatech.edu

Abstract

Heterotrophic activity, primarily driven by sulfate-reducing prokaryotes, has traditionally been linked to nitrogen fixation in the root zone of coastal marine plants, leaving the role of chemolithoautotrophy in this process unexplored. Here, we show that sulfur oxidation coupled to nitrogen fixation is a previously overlooked process providing nitrogen to coastal marine macrophytes. In this study, we recovered 239 metagenome-assembled genomes from a salt marsh dominated by the foundation plant *Spartina alterniflora*, including diazotrophic sulfate-reducing and sulfur-oxidizing bacteria. Abundant sulfur-oxidizing bacteria encode and highly express genes for carbon fixation (*RuBisCO*), nitrogen fixation (*nifHDK*) and sulfur oxidation (oxidative-*dsrAB*), especially in roots stressed by sulfidic and reduced sediment conditions. Stressed roots exhibited the highest rates of nitrogen fixation and expression level of sulfur oxidation and sulfate reduction genes. Close relatives of marine symbionts from the *Candidatus* Thiodiazotropha genus contributed ~30% and ~20% of all sulfur-oxidizing *dsrA* and nitrogen-fixing *nifK* transcripts in stressed roots, respectively. Based on these findings, we propose that the symbiosis between *S. alterniflora* and sulfur-oxidizing bacteria is key to ecosystem functioning of coastal salt marshes.

Introduction:

The microbial communities closely associated with plant hosts (i.e., plant microbiota) have received substantial attention due to their role in plant nutrient acquisition, phytohormone synthesis, prevention of soil-borne disease, and detoxification of the rhizosphere and root environment (Bulgarelli et al., 2013; Trivedi et al., 2020). Most plant microbiome studies have been performed in terrestrial ecosystems with an emphasis on agricultural plants (Trivedi et al., 2020). Plant microbiota from vegetated coastal ecosystems (i.e., seagrass meadows, mangroves, and salt marshes) remain understudied, even though they play a key role in global climate regulation and the cycling of major nutrients (Barbier et al., 2011; Duarte et al., 2013). Despite their high ecological value, little is known about how plant-microbe interactions contribute to the functioning of coastal marine ecosystems, their resilience to climate change, and provisioning of ecosystem services.

Previous studies have shown that the root zone of coastal marine plants is a hotspot for the cycling of carbon, nitrogen, and sulfur (Gandy and Yoch, 1988; Welsh et al., 1996; Spivak and Reeve, 2015; Thomas et al., 2014; Crump et al., 2018; Kolton et al., 2020). Furthermore, sulfate-reducing and sulfur-oxidizing bacteria have been shown to be overrepresented in the core root and rhizosphere microbiome of seagrass and salt marsh plants, including that of the foundation salt marsh plant *Spartina alterniflora* (Cúcio et al., 2016; Rolando et al., 2022). Sulfate reduction, an anaerobic respiration pathway, represents a dominant terminal electron-accepting process coupled to the breakdown of organic matter in marine ecosystems (Kostka et al., 2002; Jørgensen et al., 2019). Evidence from experimental and field research indicates that rhizospheric sulfate-reducing bacteria assimilate photosynthates from *S. alterniflora*, while fueling nitrogen fixation (Gandy and Yoch, 1988; Spivak and Reeve, 2015). Similarly, rates of nitrogen fixation have been closely

associated with organic matter degradation mainly by sulfate reduction in seagrass meadows (Capone, 1982; McGlathery et al., 1998; Herbert, 1999; Nielsen et al., 2001; Welsh et al., 1996). Conversely, the oxidation of reduced sulfur compounds is a chemolithotrophic process requiring terminal electron acceptors such as oxygen, nitrate, or oxidized metals. Sulfide is a known phytotoxin, and its belowground oxidation is considered a detoxifying reaction for plants inhabiting coastal marine ecosystems (Lamers et al., 2013). Based only on amplicon sequencing of the 16S rRNA gene, sulfur oxidation coupled with nitrogen fixation was recently hypothesized as an important process for plant growth under sulfidic conditions (Rolando et al., 2022). Nitrogen is often the limiting nutrient for salt marsh plants, and stress from sulfide toxicity and anoxia further impairs root active acquisition of nitrogen (Mendelssohn and Morris, 2000). Close relatives of diazotrophic sulfur-oxidizing symbionts from the *Sedimenticolaceae* family (genus: *Candidatus* Thiodiazotropha) have been shown to inhabit the roots of seagrasses and marsh plants in coastal marine ecosystems (Martin et al., 2020a, Rolando et al., 2022). The *Ca.* Thiodiazotropha genus was first discovered as bacterial symbionts of lucinid clams, where they provide both fixed carbon and nitrogen to their animal host by sulfur-mediated chemolithoautotrophy (Petersen et al., 2016; König et al., 2016). Most studies assessing the ecology and function of sulfur chemosymbiosis have been performed within marine invertebrate hosts (Petersen et al., 2016; Osvatic et al., 2021, 2023; Lim et al., 2019a, 2019b). Cúcio et al. (2018) binned genomes from four bacterial species associated with seagrass roots, including a chemolithoautotrophic sulfur-oxidizing bacteria. However, none of these genomes harbored genes for nitrogen fixation. Thus, strong evidence is lacking for the coupling of sulfur oxidation with nitrogen fixation in the roots of coastal marine plants due to the fact that the genomes, metabolic potential, and activity of diazotrophic sulfur-oxidizing bacteria have not been characterized. Limited studies have investigated the composition

and abundance of sulfur-oxidizing bacteria present in the roots of coastal marine plants. Previous studies relied on microscopy-, DNA/RNA amplicon-based community analyses or independent metagenomic and metatranscriptomic analyses (Thomas et al., 2014; Crump et al., 2018; Cúcio et al., 2018; Martin et al., 2020a; Kolton et al., 2020; Rolando et al., 2022). Because a multi-omics approach has not yet been applied to the roots of coastal plants, genome-wide gene expression profiles of uncultured sulfur-oxidizing bacteria and the coupling of sulfur oxidation with other biogeochemical processes are still to be deciphered. In addition, although the coupling of sulfate reduction to nitrogen fixation is well established in the roots of marine plants, the metabolically-active sulfate-reducers that mediate this process and their metabolic potential have not been explored with a genome-centric approach.

Ecosystem models and empirical evidence indicate that climate change is altering the hydrology, biogeochemistry, and plant community composition of coastal wetlands (Guimond et al., et al., 2020; Donnelly and Bertness, 2001; Noyce et al., 2023). Thus, a mechanistic understanding of how environmental perturbations impact plant-microbe interactions will be critical to forecasting the resilience of coastal marine ecosystems to climate change. We hypothesize that beneficial plant-microbe interactions related to plant stress amelioration will be more prevalent in plants experiencing higher levels of salinity, reduced redox conditions, and sulfide toxicity. *S. alterniflora*-dominated salt marsh ecosystems represent an ideal natural laboratory in which to study the effects of stress on plant-microbe interactions because steep gradients in plant productivity are formed within short distances (Mendelssohn and Morris, 2000). The productivity gradient is the result of decreased soil redox potential, along with increased salinity and anoxia, extending from vegetated tidal creek banks towards the interior of the marsh (Figure 1). Higher primary productivity is reflected in tall *S. alterniflora* plants (> 80 cm) growing adjacent to tidal

creek banks, while smaller plants (< 50 cm) inhabit the interior of the marsh. Furthermore, *S. alterniflora* physiological impairment along the stress gradient has been widely studied and evidenced by lower aboveground biomass and photosynthesis rates, decreased leaf area, and reduced energy status for root nitrogen uptake due to root anaerobic metabolism (Giurgevich and Dunn, 1979; Pezeshki and DeLaune, 1988; Mendelssohn and Morris, 2000). Since the root zone of the stressed short phenotype establishes an oxic-anoxic interface conducive for sulfur oxidation, we hypothesize a stronger relationship between plant roots and diazotrophic sulfur chemosymbionts. The present study closely couples biogeochemistry with a multi-omics approach to address the following objectives: (i.), to demonstrate the coupling of sulfur oxidation with nitrogen fixation in the root environment of *S. alterniflora*, (ii.) to evaluate the effect of environmental stress on the assembly, activity, and ecological interactions of the *S. alterniflora* root microbiome, and (iii.) to infer the extent of the interaction between diazotrophic sulfur-cycling bacteria in the roots of coastal marine plants.

Here, we present metagenome-assembled genomes (MAGs) from sulfate-reducing and sulfur-oxidizing bacteria that contain and highly express genes for nitrogen fixation in the roots of *S. alterniflora*. Further, we reveal that the most dominant and active sulfur-oxidizing bacteria in the *S. alterniflora* root are closely related to lucinid clam symbionts from the *Ca.* Thiodiazotropha genus. A meta-analysis of amplicon datasets from terrestrial and coastal marine ecosystems shows that seagrass meadows, salt marshes and mangroves plants assemble similar root microbiomes, with a high abundance of *Ca.* Thiodiazotropha species. Our results indicate that sulfur oxidation coupled to nitrogen fixation is a previously overlooked global process providing nitrogen to coastal marine ecosystems.

2. Results

2.1 Study site and environmental stress description

We studied the root microbiome of the salt marsh foundation species of the US Atlantic and Gulf of Mexico coastlines, *Spartina alterniflora*, at Sapelo Island, GA during the summers of 2018, 2019 and 2020. A combination of prokaryotic DNA and RNA quantification, shotgun metagenomics, metatranscriptomics, and rate measurements of nitrogen fixation were performed at two contrasting environmental conditions within three compartments: sediment, rhizosphere and root (Figure 1). The short and tall *S. alterniflora* phenotypes represent the extremes of the plant biomass gradient formed by stress from salinity, sulfide toxicity and anoxia (Figure 1). Four biological replicates per compartment and *S. alterniflora* phenotype were sequenced for both metagenomic and metatranscriptomic analysis. Rhizosphere samples were only used for metagenomic analysis due to limited samples for RNA extractions (Further details regarding sequencing can be found in the Methods section and Supplementary Data File S1).

Sediment and root microbiomes showed contrasting diversity, abundance, and functional profiles in both *S. alterniflora* phenotypes. Prokaryotic alpha diversity was greater in the sediment and rhizosphere compared to the root compartment in both *S. alterniflora* phenotypes (Figure 2a). Similarly, quantification of the 16S rRNA gene by qPCR showed statistically lower prokaryotic abundance in root tissue compared to the sediment and rhizosphere (Figure 2a). A stronger barrier for prokaryotic root colonization, evidenced by a steeper decrease in prokaryotic abundance in the rhizosphere-root interface, was observed in the less stressed tall *S. alterniflora* phenotype (Figure 2a). Conversely, the root compartment of both *S. alterniflora* phenotypes presented a higher transcript copy number of the prokaryotic 16S rRNA than their sediment counterparts, indicating greater prokaryotic activity in the root zone (Figure 2a). PERMANOVA and principal coordinate analysis of metagenomic and metatranscriptomic functional profiles indicate that environmental

159 stress significantly affected the microbiome's potential and expressed functional repertoire (Figure
160 2b, Supplementary Table S1). Differences in potential and expressed functional metabolism were
161 evidenced in terminal oxidases and biogeochemical pathways in the carbon, nitrogen, and sulfur
162 cycles (Supplementary Figure S1).

163 2.2 Genome-centric multi-omics approach reveals prokaryotic sulfur metabolism is coupled to
164 nitrogen fixation in the roots of a foundation salt marsh plant

165 Using a custom-designed bioinformatics pipeline, we binned 239 metagenome assembled
166 genomes (MAGs). Only MAGs with greater than 50 quality score (QS: Completeness –
167 5*Contamination) were retained. The 16S rRNA gene was binned in 68 of the 239 MAGs
168 (Supplementary Data File S2). MAGs were dereplicated into 160 genomospecies (gsp, plural:
169 gspp) by grouping them according to 95% average nucleotide identity (ANI) (Figure 3). The
170 median percentage of non-eukaryotic short reads mapping back to MAGs was 6% and 22% in the
171 tall and short roots, respectively. High prokaryotic diversity and sequencing of eukaryotic DNA
172 prevented the assembly and binning of a large diversity still to be described in this ecosystem.
173 MAGs were assigned to 19 phyla. Almost half of the recovered genomes were taxonomically
174 affiliated with the *Proteobacteria* or *Desulfobacterota* phyla (Figure 3, further MAGs taxonomic
175 and statistical information in Supplementary Data File S2). Taxonomic novelty was assessed using
176 GTDB-Tk v2.1.0 with the reference database R07-RS207 (Chaumeil et al., 2022). Recovered
177 MAGs included 1 gspp from a previously undescribed order, 10 gspp from undescribed families,
178 52 gspp from undescribed genera, 94 gspp from undescribed species, and only 3 gspp from
179 previously described species. In order to assess the MAGs' genetic potential to perform important
180 biogeochemical functions in the salt marsh environment, we annotated their open reading frames

(ORFs) using the eggNOG database, and focused on predicted genes involved in the biogeochemical cycling of carbon, nitrogen, and sulfur (Supplementary Data File S3).

A large proportion of binned *Proteobacteria*, including members of the *Ca.* Thiodiazotropha genus, contained genes for nitrogen fixation, carbon fixation through RuBisCO, as well as for dissimilatory sulfur metabolism, and thiosulfate oxidation using the soxABXYZ complex (Figure 3). Most MAGs from the *Desulfobacterota* phylum presented genes for dissimilatory metabolism of sulfur, including members of the *Desulfosarcinaceae* family (Figure 3). Because the dissimilatory sulfite reductase enzyme (dsrAB) can function in either sulfur reduction or oxidation, we performed a phylogenetic analysis to identify the dsrAB type encoded in our MAGs. We aligned recovered *dsrAB* genes to a reference alignment (Müller et al., 2015) and annotated the *dsrAB* type based on placement in an approximately-maximum-likelihood phylogenetic tree (Supplementary Figure S2). All *dsrAB* genes retrieved from *Proteobacteria* gspp (*Alpha*- and *Gammaproteobacteria* gspp) were placed within the oxidative type; while *dsrAB* genes recovered from *Acidobacteriota*, *Bacteroidota*, *Chloroflexota*, *Desulfobacterota*, *Gemmatimonadota*, and *Nitrospirota* gspp clustered within the reductive bacterial *dsrAB* type (Supplementary Figures S2, S3).

We measured rates of N fixation under oxic and anoxic conditions in sediment, a rhizosphere-root mix, and root samples using the $^{15}N_2$ stable isotope tracing technique. Rates were measured under oxic and anoxic conditions to capture the oxygen fluctuation experienced by microorganisms in the root-zone of *S. alterniflora*. The two *S. alterniflora* phenotypes exhibited significantly higher N fixation rates in their root tissue compared to the sediment or rhizosphere-root mix under both aerobic and anaerobic conditions (Figure 4a). Root tissue from the stressed short *S. alterniflora* phenotype showed 1.9- and 5.1-times greater N fixation rates than roots of the tall phenotype under

aerobic and anaerobic conditions, respectively (Figure 4a). In addition, natural abundance isotopic composition revealed a depletion of $\delta^{15}N$ in the short phenotype compared to the tall phenotype in all assessed compartments, providing further evidence of greater nitrogen fixation in this zone of the marsh (Figure 4a).

We used metagenomic and metatranscriptomic short reads to relate nitrogen fixation activity with multi-omics functional information. Metagenomic and metatranscriptomic reads were functionally annotated using the eggNOG database. We normalized the functional profile of each library to account for differences in sequencing effort and genome size by dividing the count matrix against the median abundance of 10 universal single-copy phylogenetic marker genes as in Salazar et al. (2019). Statistical difference between the normalized gene expression of the nitrogenase gene *nifK* and the oxidative and reductive *dsrA* types was calculated between *S. alterniflora* phenotypes across all compartments. Since gene expression within metabolic pathways was highly correlated, we used *nifK* and *dsrA* as marker genes (Supplementary Figure S4). Even though nitrogen fixation rates were the greatest in the root compartment of the short *S. alterniflora* phenotype, no statistical significance was found in the nitrogenase gene expression between the two phenotypes (Figure 4b). Conversely, the root compartment of the short *S. alterniflora* phenotype had the highest normalized transcript abundance of both reductive and oxidative *dsrA* gene types (Figure 4b). To infer which members of the *S. alterniflora* root microbiome contributed the most to nitrogen fixation, as well as to test if nitrogen fixation was coupled to sulfur metabolism, we mapped all metatranscriptomic short reads annotated as *nifK* and *dsrA* back to our MAGs as well as ORFs from assembled but not binned scaffolds. Sulfur-oxidizing *Ca.* Thiodiazotropha unbinned scaffolds and gspp (i.e., dereplicated MAGs) in the short phenotype of *S. alterniflora* contributed approximately 30% and 20% of all oxidative *dsrA* and *nifK* functionally-annotated short reads,

227 respectively (Figure 4c). In addition, the most active sulfur-oxidizing and sulfate-reducing gspp in
228 roots of the short phenotype (gsp 31 and gsp 68) had a positive correlation between nitrogen
229 fixation and sulfur oxidation/reduction gene expression, respectively (Supplementary Figure S5,
230 Supplementary Figure S6). In the tall phenotype, *Desulfosarcinaceae* gsp 134, and unbinned
231 scaffolds from the *Deltaproteobacteria* class and *Desulfatitalea* genus contributed the most
232 transcripts of the reductive *dsrA* gene (Figure 4c). However, in the tall phenotype we were not able
233 to map most *nifK* transcripts to MAGs, due to high diversity preventing assembly and binning.
234 Nevertheless, using short read analysis, we found that the majority of the *nifK* transcripts in the
235 roots of the tall phenotype were assigned to bacteria from the *Desulfobacterota* phylum, while in
236 the short phenotype most *nifK* transcripts were affiliated with bacteria from the
237 *Gammaproteobacteria* class or the *Desulfobacterota* phylum (Supplementary Figure S7).
238 Oxidative *dsrA* transcripts in the roots of the short phenotype were mostly affiliated with the
239 *Gammaproteobacteria* class, while the reductive *dsrA* affiliated mainly with the *Desulfobacterales*
240 and *Desulfovibrionales* orders in both phenotypes (Supplementary Figures S8 and S9). Similarly,
241 16S rRNA amplicon analysis from the same sample set used for metatranscriptomic analysis
242 showed the highest transcript abundance of gammaproteobacterial *Ca.* Thiodiazotropha in the
243 roots of the short *S. alterniflora* phenotype when compared to the sediment of the two phenotypes
244 and root of the tall phenotype (Supplementary Figure S10).

245 2.3 Phylogeny, genetic potential and gene expression of microorganisms enriched in the *S.*
246 *alterniflora* root microbiome

247 To assess the phylogenetic novelty and relation of *Sedimenticolaceae* sulfur-oxidizing MAGs from
248 the present study in comparison to that of marine invertebrate chemosymbionts, we retrieved all
249 publicly available *Sedimenticolaceae* genomes as reported by GTDB release R07-RS207, as well

as all *Ca.* Thiodiazotropha spp. analyzed by Osvatic et al. (2023). A maximum-likelihood phylogenetic tree using 382 genes from a 400 universal marker genes database was performed in PhyloPhlAn. The phylogenetic tree used a concatenated alignment containing 14,693 amino-acid positions. We found that *S. alterniflora* root symbionts assigned to the *Ca.* Thiodiazotropha genus and an unknown genus from the *Sedimenticolaceae* family formed a monophyletic clade with lucinid clam chemosymbionts (Figure 5). All recovered MAGs that were phylogenetically related to marine invertebrate chemosymbionts were highly abundant in the root compartment of the *S. alterniflora* short phenotype, where sulfidic conditions are found in the marsh environment (Figure 1). To conserve phylogenetic coherence, we propose that *S. alterniflora* root symbionts assigned to the *Sedimenticolaceae* family and that formed a monophyletic group with *Ca.* Thiodiazotropha spp. are also members of this genus (Figure 5). All *Ca.* Thiodiazotropha symbionts of *S. alterniflora* are distinct species from those previously found in lucinid clam hosts (ANI < 82% for all pairwise comparisons). Out of the 7 recovered *Ca.* Thiodiazotropha gspp, 6 had genes for carbon fixation (*RuBisCO*), 5 had the complete or partial *nifHDK* nitrogenase genes for nitrogen fixation, and all of them harbor the complete or at least partial genes for dissimilatory sulfite reductase (oxidative *dsrAB* type), and sulfur oxidation by the SOX complex (*soxABXYZ*). All of the *Ca.* Thiodiazotropha gspp contained genes for carbon metabolism through the TCA cycle, and only two *Ca.* Thiodiazotropha gspp harbored genes for nitrate reduction (gsp 32 and gsp 33). It is possible, however, that the absence of functional genes in recovered MAGs is due to the incomplete nature of the genomes.

We calculated the gene expression profile of the most active *Ca.* Thiodiazotropha gspp (gsp 31 and gsp 33), finding that genes for sulfur oxidation through the oxidative *dsrAB*, *soxABXYZ* complex, and cytochrome c oxidase cbb3-type genes, as well as genes for carbon and nitrogen

fixation (*RuBisCO* and *nifHDK*) were among the most highly transcribed (Supplementary Data Files S4 and S5). Microaerophilic oxygen reductases (i.e., cytochrome c oxidase cbb3-type and cytochrome bd ubiquinol oxidase) showed higher transcript levels compared to nitrate reductase in gsp 33 (Supplementary Data File S5).

We also found that sulfate-reducing MAGs from the *Desulfosarcinaceae* family were enriched in the root compartment of *S. alterniflora* (Supplementary Figure S11). *Desulfosarcinaceae* gspp had contrasting preferences for root colonization, with gsp 68 mostly enriched in the roots of the short phenotype, gsp 134 preferentially enriched in the root of the tall phenotype, and gsp 80 equally abundant in both phenotypes (Supplementary Figure S11). Of the three *Desulfosarcinaceae* gspp, all contained the complete or partial genes for nitrogen fixation, and only gsp 80 did not have the reductive *dsrAB* gene. The most transcribed genes from both gsp 68 and gsp 134 were related to dissimilatory sulfate reduction (*dsrAB* and *aprAB*, Supplementary Data Files S6 and S7).

2.4 Plant species from coastal marine ecosystems harbor unique root microbiomes

We compiled and curated a 16S rRNA gene amplicon database from root microbiomes comprising 2,911 amplicon samples from 56 plant species (complete dataset in Supplementary Data File S8). Our aim was to assess the applicability of our study's findings to global coastal vegetated ecosystems and to compare the assembly of root microbiomes in coastal marine macrophytes to that of well-studied terrestrial plants. We grouped amplicon samples into 4 broad ecosystem types: seagrass meadows, coastal wetlands (i.e., salt marshes and mangroves), freshwater wetlands, and terrestrial ecosystems. Species exchange based on the Bray-Curtis dissimilarity indices was largely explained by ecosystem type, with coastal wetland and seagrass meadow plants clustering together in an NMDS ordination (Figure 6a). PERMANOVA analysis revealed that ecosystem type alone significantly explained 13.2% of the variation of the species exchange between analyzed samples

(Supplementary Table S2). Furthermore, to explore two functional guilds that may explain the difference in microbiome assembly among ecosystem types, we assigned putative sulfate reduction and sulfur oxidation functions to our taxonomy table as performed by Rolando et al. (2022). Putative function was inferred based on homology at the genus level with prokaryotic species with known sulfur oxidation or sulfate reduction metabolism (Supplementary Data File S9). We found that the root microbiomes of both seagrass meadow and coastal wetland ecosystems were highly enriched in putative sulfate-reducing and sulfur-oxidizing bacteria (Figure 6b, 6c). Furthermore, we discovered that in both seagrass meadows and coastal wetland ecosystems, amplicons showing high sequence identity to sulfur-oxidizing bacteria with the capability for nitrogen fixation (*Sedimenticolaceae* family: *Ca.* Thiodiazotropha genus) were highly abundant (Supplementary Figure S12). In addition, amplicons showing high sequence identity to sulfate reducers from the *Desulfosarcinaceae* family, particularly those from the genus *Desulfatitalea,* were highly enriched in the roots of coastal wetland plants (Supplementary Figure S12). The taxonomic identity of highly abundant ASVs in the root compartment of coastal marine plants match those of diazotrophic MAGs retrieved from Sapelo Island, GA, such as sulfur oxidizers of the *Sedimenticolaceae* family, and sulfate reducers of the *Desulfosarcinaceae* family.

3. Discussion

Nitrogen fixation in belowground coastal vegetated ecosystems has been mainly associated with heterotrophy, and particularly with sulfate reduction (Gandy and Yoch, 1988; McGlathery et al., 1998; Herbert, 1999; Nielsen et al., 2001; Welsh et al., 1996). The linkage of sulfate reduction to nitrogen fixation was proposed based on studies quantifying rates of diazotrophy with and without sulfate reduction inhibition by molybdate (Capone, 1982; McGlathery et al., 1998; Nielsen et al., 2001; Welsh et al., 1996). Here, we show that highly-abundant sulfur-oxidizing bacteria in the

roots of *S. alterniflora* also encode and highly express genes for nitrogen fixation. Furthermore, the MAG with the highest nitrogenase gene expression in our study is a novel sulfur-oxidizing bacterium from the *Ca.* Thiodiazotropha genus that also showed high expression of sulfur oxidation genes. It is possible that when sulfate reduction was inhibited in previous studies (McGlathery et al., 1998; Nielsen et al., 2001; Welsh et al., 1996), it disrupted the redox cycling of sulfur by impeding the flow of reduced sulfur for bacterial sulfur oxidation. Thus, not only was nitrogen fixation mediated by sulfate-reducing microorganisms inhibited, but also nitrogen fixation coupled to sulfur oxidation was likely impaired. Further evidence supporting the significance of the cycling of sulfur on nitrogen fixation is that members of the *Gammaproteobacteria* class and *Desulfobacterota* phylum contributed the majority of nitrogenase and oxidative/reductive *dsrAB* transcripts in the root compartment of *S. alterniflora*. Previous work employing DNA and RNA amplicons or short read 'omics analysis in seagrass and other coastal wetland plant species, showed nitrogen fixation genes and their expression to be affiliated with microorganisms closely related to sulfate-reducing and sulfur-oxidizing bacteria (Thomas et al., 2014; Crump, et al. 2018; Kolton et al., 2020). However, very few genomes for these sulfur cycling organisms were available and a genome-centric analysis had not yet been applied. Here, we present MAGs from diazotrophic sulfate-reducing and sulfur-oxidizing bacteria that highly express genes for both nitrogen fixation and dissimilatory sulfur reactions. Thus, we propose that both dissimilatory sulfur reduction and oxidation, and more importantly, the rapid redox cycling of sulfur, stimulate nitrogen fixation in the root environment of *S. alterniflora*. Since we show that coastal wetland plants and seagrasses assemble similar root microbiomes, and macrophyte activity boosts both nitrogen fixation and the cycling of sulfur, this is most likely a common phenomenon

in the root zone of coastal marine plants worldwide (Whiting et al., 1986; McGlathery et al., 1998; Welsh et al., 1996; Fahimipour et al., 2017).

In most coastal marine ecosystems, water saturated sediments are often depleted in oxygen within the first few millimeter's depth (Jørgensen et al., 2019). Because coastal marine ecosystems are bathed in seawater containing high sulfate concentrations (28 mM), sulfate-reducing microorganisms often perform the terminal step of organic matter decomposition (Jørgensen et al., 2019). Unlike aerobic respiration, energy flow during sulfate reduction is decoupled from the carbon cycle, with most of the free energy conserved in reduced sulfur compounds (Howarth, 1984). The chemically stored energy is subsequently released by biotic and abiotic oxidation reactions at oxic-anoxic interfaces coupled to the reduction of electron acceptors (oxygen, nitrate, or oxidized metals) (Howarth, 1984). Surface sediments of vegetated coastal marine ecosystems experience rapid re-oxidation of most reduced sulfur compounds. This process is highly concentrated in the microaerophilic root zone, which serves as a hotspot for the reaction (Holmer et al., 2002; Kristensen and Alongi, 2006; Koop-Jakobsen et al., 2018). Our results showing that the root compartment of coastal marine ecosystems is highly enriched in microorganisms with the capability for both sulfur reduction and oxidation provides further evidence for rapid sulfur cycling in the root zone. Furthermore, to the best of our knowledge, this is the first study to employ a multi-omics approach to reconstruct genomes and determine gene expression of uncultivated sulfate-reducing and sulfur-oxidizing microorganisms living in the roots of coastal wetland plants. Our findings also reveal that genes that catalyze oxidative and reductive reactions in the sulfur cycle along with those of nitrogen fixation are highly transcribed in the root environment, particularly in the stressed *S. alterniflora* phenotype that thrives in a sulfidic environment (Rolando et al. 2022). This is consistent with previous studies of salt marsh and seagrass ecosystems, in

364 which genes of sulfur-oxidation pathways were shown to be highly expressed in the root
365 compartment of *S. alterniflora* and *Zostera* seagrass spp., respectively (Thomas et al. 2014, Crump
366 et al., 2018). Thus, we propose that in contrast to terrestrial ecosystems, coastal marine plants rely
367 on the rapid cycling of sulfur in their root zone for the breakdown of organic matter and recycling
368 of nutrients through sulfate reduction along with the re-oxidation of terminal electron acceptors by
369 sulfur oxidation. Furthermore, we propose that rapid rates of both oxidative and reductive sulfur
370 reactions represent a key mechanism to sustain high rates of energetically-expensive nitrogen
371 fixation in the root zone of coastal wetland and seagrass plants.

372 In this study, we reveal the genomes, phylogeny, function, and gene expression of
373 chemolithoautotrophic symbionts discovered in the roots of *S. alterniflora*. Endosymbionts from
374 the *Ca.* Thiodiazotropha genus were initially discovered living in symbiosis with lucinid clams,
375 where they fix carbon and serve as a source of carbon and nitrogen to the animal host using energy
376 gained from the oxidation of reduced forms of sulfur (Petersen et al., 2016). Recent studies using
377 fluorescence in situ hybridization (FISH) microscopy and SSU rRNA gene metabarcoding have
378 shown that *Ca.* Thiodiazotropha bacteria also inhabit the roots of a diverse array of seagrass species
379 along with that of the coastal cordgrass *S. alterniflora* (Martin et al., 2020a; Rolando et al., 2022).
380 Here, we show that close relatives of diazotrophic sulfur chemosymbionts associated with lucinid
381 clams were highly abundant and active in the roots of *S. alterniflora*. We report genomes and gene
382 expression profiles from *Ca.* Thiodiazotropha retrieved from macrophyte root samples and show
383 that our MAGs formed a monophyletic clade with those from previously described marine
384 invertebrate animals. Similar to what has been reported in their symbiosis with lucinid clams, the
385 *S. alterniflora* symbionts highly expressed genes for sulfur oxidation, carbon fixation, and nitrogen
386 fixation (Petersen et al., 2016; Lim et al., 2019a). However, the presence and expression of genes

for glycolysis and the TCA cycle point to a mixotrophic lifestyle, akin to what is observed in their symbiosis with lucinid clams (Petersen et al., 2016; Lim et al., 2021). High expression of high-affinity oxygen reductases, such as the cytochrome c oxidase cbb3-type and cytochrome bd ubiquinol oxidase, may serve as adaptations for oxygen respiration under sulfidic conditions as well as an oxygen scavenging strategy for nitrogen fixation (Dincturk et al., 2011; Borisov et al., 2021). Moreover, the fluctuation of the redox state in the root zone of macrophytes during diel and tidal cycles may influence how *Ca.* Thiodiazotropha gspp partition aerobic and anaerobic metabolic processes (Taillefert et al., 2007; Koop-Jakopsen et al., 2018; Marzocchi et al., 2019). Further investigation is warranted to uncover the biogeography, host specificity, and temporal dynamics of *Ca.* Thiodiazotropha in association with macrophyte roots.

Studies of lucinid clams have shown that the *Ca.* Thiodiazotropha symbionts are horizontally transmitted (Petersen and Yuen, 2021). Furthermore, invertebrate colonization by *Ca.* Thiodiazotropha symbionts is not restricted by either the host or symbiont species (Lim et al., 2019a). The flexibility of this symbiotic relationship could explain the evolution of *Ca.* Thiodiazotropha colonization in macrophyte roots. Previous studies have suggested that the root zone of seagrass species serves as a reservoir of chemosymbionts for marine invertebrates (Cúcio et al., 2018). However, our studied marsh lacks lucinid clams or any marine invertebrate known to harbor bacterial chemosymbionts. Further, application of a genome-centric approach to both macrophyte plant and lucinid clam hosts is needed to better interrogate if chemosymbiont populations are restricted by host biology at the kingdom level (i.e., to either plant or animal hosts), or if symbionts are shared and horizontally transferred between plant and invertebrate species. In contrast to what is observed in lucinid clams, where a single or few bacterial species dominates the gill microbiome; in *S. alterniflora* and seagrass species, *Ca.* Thiodiazotropha spp. do not

outcompete other microbial species in the root compartment (Lim et al., 2019a, 2019b). However, the symbionts comprise a large proportion of the microbial community, and are amongst the most active species (Rolando et al., 2022).

We propose that the symbiosis between *S. alterniflora* and sulfur-oxidizing bacteria represents a key adaptation supporting the resilience of coastal salt marsh ecosystems to environmental perturbations. Intertidal wetland ecosystems are vulnerable to climate change because they are located in a narrow elevation range determined by tidal amplitude (Morris et al., 2021). The Intergovernmental Panel on Climate Change (IPCC) has projected an increase in sea level between 0.38 m and 0.77 m by 2100 (IPCC-AR6, Fox-Kemper et al., 2021). Although coastal wetland ecosystems are dynamic and adapt to sea level rise by increasing sediment accretion rates, ecosystem models predict that a large area of present-day marsh will drown because of accelerated sea level rise (Kirwan et al., 2016). Increased hydroperiods will impact the redox balance of vegetated sediments, imposing more severe anoxia and physiological stress from sulfide toxicity to wetland plants. Under this scenario, a symbiosis of coastal vegetated plants with sulfur-oxidizing bacteria could alleviate sulfide stress while at the same time coupling it to carbon and nitrogen fixation for potential plant uptake. However, the mechanism for carbon and/or nitrogen transfer between sulfur-oxidizing symbionts and the host plants still remains elusive and requires further research. Similar to Thomas et al. (2014), we showed the transcription of sulfur oxidation genes was greater in the stressed *S. alterniflora* short phenotype. In seagrass ecosystems, Martin et al. (2020b) also found that the seagrass root microbiome was more enriched in *Ca.* Thiodiazotropha spp. under stress conditions. Thus, we suggest that the *S. alterniflora* – *Ca.* Thiodiazotropha symbiosis is an adaptive interaction to anoxic soil conditions, whereby the host plant responds to stress from elevated dissolved sulfide concentrations. Further, we show that the

short *S. alterniflora* phenotype, which harbors a greater nitrogenase transcript abundance of *Ca.* Thiodiazotropha chemosymbionts, also displayed the greatest rates of N fixation of all assessed marsh compartments. Stressed plants benefit from the symbiotic relationship through reduced sulfide toxicity and the coupling of sulfide oxidation to nitrogen fixation, with nitrogen likely transferred to the plant host. Conversely, the tall *S. alterniflora* phenotype showed a greater expression of genes involved in the internal cycling of nitrogen, which is consistent with previous studies showing greater rates of nitrogen mineralization in this zone of the ecosystem (Rolando et al., 2022).

4. Methods

4.1 Study site, field sampling and sample processing

All field sampling was performed within the United States in the state of Georgia. Sampling was performed with authorization from the Georgia Department of Natural Resources (File: LOP20190067). Specifically, we sampled salt marsh ecosystems within the Georgia Coastal Ecosystem - Long Term Ecological Research (GCE-LTER) site 6, located on Sapelo Island, GA (Lat: 31.389° N, Long: 81.277° W). Four ~100 m transects along the tall to short *Spartina alterniflora* gradient were studied in July 2018, 2019, and 2020 (Figure 1, further site description in Rolando et al., 2022). A combination of multi-omics approaches and biogeochemical rate measurements were performed across different salt marsh compartments and phenotypes of *S. alterniflora*.

The microbiome of *S. alterniflora* was analyzed using shotgun metagenomics from three compartments: sediment, rhizosphere, and root. The tall and short *S. alterniflora* extremes of the four studied transects were sampled (n: 4 transects * 2 *S. alterniflora* phenotypes * 3 compartments

455 = 24). Samples from transects 1 and 2 were collected in July 2018, while those from transects 3
456 and 4 were collected in July 2019. All sampling was performed at the 0-5 cm depth profile. Root-
457 associated samples were washed two times with creek water in the field to remove coarse chunks
458 of sediment attached to the plant. All samples were immediately flash-frozen in an ethanol and dry
459 ice bath, and stored at -80ºC until DNA extraction.

460 Samples for metatranscriptomic analysis and biogeochemical rate measurements were collected in
461 July 2020 only from transect 4 to reduce plant disturbance time before flash freezing and
462 incubations, respectively. Five independent plants at least 3 meters apart were sampled with a
463 shovel at the two *S. alterniflora* biomass extremes. Sampling was performed in the morning (~9:00
464 am) during low tide. A 25-cm diameter marsh section including several *S. alterniflora* shoots,
465 undisturbed root system, and sediment was sampled up to at least 20 cm depth and transferred to
466 a 5 gallons bucket. Plant samples were immediately transported to the field lab with no evidence
467 of physiological stress noted after sampling. For each plant, a paired sample of sediment was
468 collected. In the lab, roots were washed with creek water two times. After the first wash, roots with
469 sediment attached were collected and defined as the rhizosphere + root compartment. Live,
470 sediment-free roots were sampled after the second wash and defined as the root compartment. Top
471 5 cm from each sample were homogenized and used for total RNA extractions and measurements
472 of nitrogen fixation rates. Root samples for RNA extractions were washed in an epiphyte removal
473 buffer in ice, as in Simmons et al. (2018). Sediment and root samples for RNA analysis were
474 immediately flash-frozen in an ethanol dry ice bath, and stored at -80 ºC until extraction. Total
475 root processing time since washing to flash-freezing was about 1.5 hours due to *S. alterniflora*
476 intertwined root system with plant debris. Due to limited sample amount, we did not prepare
477 rhizosphere libraries for metatranscriptomic analysis.

478 4.2 Nitrogen fixation rates

479 Rates of N fixation were calculated in $^{15}N_2$ incubations in 14 ml serum vials as in Leppänen et al.
480 (2013). Rate measurements were started at the same day of plant collection, within 8 hours after
481 plant sampling. Rates were measured for all samples under both oxic and anoxic conditions. About
482 2 g, and 1 g of wet weight was used for tracer gas incubations of sediment and root samples,
483 respectively. An additional subsample of 2 g was immediately oven-dried at 60 ºC for 72 hours to
484 be used as a pre-incubation control. In all vials containing root samples, 4 ml of autoclaved and
485 0.22 µm filter-sterilized artificial seawater was added to avoid tissue desiccation. No artificial
486 seawater was added to sediment and rhizosphere samples since they were already water-saturated.
487 In anoxic incubations, vials were flushed with N_2 gas for 5 minutes. After sealing all incubation
488 vials, 2.8 ml of gas was removed and immediately replaced with 2.8 ml of $^{15}N_2$ (98% enriched,
489 Cambridge Isotope Laboratories Inc, USA). Vials were overpressured by adding 0.3 ml of air or
490 N_2 gas in oxic or anoxic incubations, respectively. The incubations were carried out in the dark
491 and at room temperature for 24 hours. At the end of the incubation, samples were oven dried at 60
492 ºC for 72 hours, and ground using a PowerGen high throughput homogenizer (Fisherbrand,
493 Pittsburgh, PA). Ground samples were sent to the University of Georgia Center for Applied Isotope
494 Studies (https://cais.uga.edu/) for carbon and nitrogen elemental analysis and ^{13}C and ^{15}N stable
495 isotope analysis. Elemental analysis was performed by the micro-Dumas method, while isotopic
496 analysis by isotope ratio mass spectrometry. Rates of ^{15}N incorporation were calculated per dry
497 weight basis (DW) as in Leppänen et al. (2013):

498 N uptake rate $\left(\text{nmol g}^{-1}\text{ DW h}^{-1}\right)=$

499
$$\frac{\frac{1}{100}\times\frac{\%N}{100}\times\left[\frac{\text{atom\%}_{\text{sample}}\text{-atom\%}_{\text{control}}}{MW(N_2)}\right]\times10^9\times\frac{100}{\text{atom\%}_{\text{headspace}}}}{\text{hours}} \qquad [1]$$

500 Where %N is the N percent concentration of the oven-dried sample, and MW(N_2) is the molecular
501 weight of N_2 (28.013446).

502 4.3 Nucleic acid extractions and multi-omics library preparation

503 For DNA extractions, compartment separation of the rhizosphere and root microbiomes was
504 performed by sonication in an epiphyte removal buffer, as detailed in Simmons et al. (2018).
505 Extracellular dissolved or sediment-adsorbed DNA was removed from bulk sediment samples
506 according to the Lever et al. (2015) procedure. DNA extractions from all samples were performed
507 using the DNeasy PowerSoil kit (Qiagen, Valencia, CA) following the manufacturer's instructions.
508 Shotgun metagenome sequencing was performed on an Illumina NovaSeq 6000 S4 2x150 Illumina
509 flow cell at the Georgia Tech Sequencing Core (Atlanta, GA).

510 RNA from 4 biological replicates of both the sediment and root compartments from the tall and
511 short phenotypes of *S. alterniflora* was extracted using the ZymoBIOMICS RNA Miniprep (Zymo
512 Research Corp) kit according to the manufacturer's protocol (n: 4 replicates * 2 *S. alterniflora*
513 phenotypes * 2 compartments = 16 samples). Rigorous DNA digestion was done with the TURBO
514 DNase kit (Invitrogen), and eukaryotic mRNA was removed by binding and discarding the
515 eukaryotic mRNA polyA region to oligo d(T)25 magnetic beads (England Biolabs). Finally, rRNA
516 from both plant and prokaryotic organisms was depleted using the QIAseq FastSelect -rRNA Plant,
517 and -5S/16S/23S kits, respectively (Qiagen, Valencia, CA). Metatranscriptomic libraries were
518 sequenced in two lanes of Illumina's NovaSeq 6000 System flow cell utilizing the NovaSeq Xp
519 workflow (SE 120bp) at the Georgia Tech Sequencing Core (Atlanta, GA). We retrieved 203, and
520 415 Gpb of metagenomic and metatranscriptomic raw sequences, respectively; with a median
521 sequencing effort of 7.8, and 25.3 Gbp per metagenomic and metatranscriptomic library
522 (Supplementary Data File S1). After quality control and *in silico* removal of host and rRNA reads,

median sequencing effort decreased to 5.2 and 8.3 Gbp per metagenomic and metatranscriptomic library, respectively (Supplementary Data File S1).

4.4 Gene and transcript quantification of the prokaryotic 16S rRNA gene

Prokaryotic abundance and a proxy of prokaryotic activity were measured by quantitative polymerase chain reaction (qPCR) and Reverse Transcription-qPCR (RT-qPCR) of the SSU rRNA gene, respectively. All samples used for metagenome and metatranscriptome analysis were quantified by qPCR and RT-qPCR, respectively. Samples were analyzed in triplicate using the StepOnePlus platform (Applied Biosystems, Foster City, CA, USA) and PowerUp SYBR Green Master Mix (Applied Biosystems, Foster City, CA, USA). Reactions were performed in a final volume of 20µl using the standard primer set for the prokaryotic SSU rRNA gene: 515F (5′-GTGCCAGCMGCCGCGGTAA′) and 806R (5′-GGACTACHVGGGTWTCTAAT′) (Caporaso et al., 2011, Rolando et al., 2022). To avoid plant plastid and mitochondrial DNA/cDNA amplification from root samples, peptide nucleic acid PCR blockers were added to all qPCR and RT-qPCR reactions at a concentration of 0.75 µM (Lundberg et al., 2013). Standard calibration curves were performed using a 10-fold serial dilution (10^3 to 10^8 molecules) of standard pGEM-T Easy plasmids (Promega, Madison, WI, USA) containing target sequences from *Escherichia coli* K12. Melting curve analyses was used to check for PCR specificity. Prokaryotic gene and transcript abundance of the SSU rRNA gene were calculated as gene and transcript copy number g^{-1} of fresh weight, respectively.

4.5 Metagenomic and metatranscriptomic quality control

Metagenomic and metatranscriptomic raw reads were quality trimmed (quality phred score < 20), and filtered for Illumina artifacts, PhiX, duplicates, optical duplicates, homopolymers, and

heteropolymers using JGI's BBTools toolkit v.38.84 (Bushnell, 2014). Reads shorter than 75 bp were removed, and the quality of both metagenomic and metatranscriptomic libraries was assessed with FastQC (Andrews, 2010). Remaining reads were mapped against the only publicly available *S. alterniflora* genome (NCBI BioProject: PRJNA479677) with bowtie2 v.2.4.2 (Langmead and Salzberg, 2012), followed by removal of short reads that aligned to the *S. alterniflora* genome using samtools (parameters: view -u -f 12 -F256, Li et al., 2009). In addition, rRNA reads from metatranscriptomic samples were removed using sortMeRNA v.4.3.4 (Kopylova et al., 2012). Finally, DNA contamination in metatranscriptomic samples was assessed as indicated by Johnston et al. (2019). Short-read transcripts were mapped to all assembled contigs, and strand-specificity (consistency in sense/antisense orientation) was calculated for all genes with more than 100 hits. All assessed samples had a greater than 95% average strand-specificity; thus, considered to be free of DNA contamination (Supplementary Data File S1). Filtered, quality-trimmed, and host-free reads were utilized for subsequent analyses.

4.6 Metagenomic and metatranscriptomic short reads functional analysis and nonpareil diversity

Short reads from all metagenomic and metatranscriptomic samples were aligned against the eggNOG protein database (release 5.0.2) using eggnog-mapper v.2.1.9 (Cantalapiedra et al., 2021). The DIAMOND tabular outputs were filtered by retrieving only the best hit based on bitscore. Hits with less than 30% identity, less than 30% match of the read length, or that did not match a prokaryotic domain were removed from the analysis. Gene profiles for each metagenomic and metatranscriptomic library were constructed by counting hits of predicted KEGG orthology. Due to differences in sequencing effort and genome size between multi-omics libraries, the count matrixes were normalized by dividing them by their median count of 10 universal single-copy phylogenetic marker genes (K06942, K01889, K01887, K01875, K01883, K01869, K01873,

K01409, K03106, and K03110) as in Salazar et al. (2019). Functional gene and transcript profiles were analyzed by principal coordinate analysis utilizing the Bray-Curtis dissimilarity distance. Further, for both metagenomic and metatranscriptomic profiles, multivariate variation of the Bray-Curtis dissimilarity matrix was partitioned to compartment (sediment, rhizosphere, and root) and *S. alterniflora* phenotype, based on a permutational multivariate analysis of variance (PERMANOVA) with 999 permutations performed in vegan v. 2.5.7 (Oksanen et al., 2013). The normalized relative abundance of selected terminal oxidases and genes/transcripts from the carbon, nitrogen, and sulfur cycles were assessed by compartment and *S. alterniflora* phenotype.

After removing reads annotated as Eukaryotic by eggnog-mapper, we calculated nonpareil diversity from all metagenomic samples using nonpareil v. 3.401 (Rodriguez-R et al., 2018b). Nonpareil diversity is a metric estimated from the redundancy of whole genome sequencing reads, and has been shown to be closely related to classic metrics of microbial alpha diversity such as the Shannon index.

4.7 Recovery of metagenome assembled genomes (MAGs)

The following binning approach was motivated by a recently proposed method of iteratively subtracting reads mapping to MAGs, re-assembling, and re-binning metagenomic libraries to increase the number of recovered genomes (Rodriguez-R et al., 2020). An initial assembly using idba-ud v1.1.3 with pre-error-correction for highly uneven sequencing depth was performed for all individual metagenomic libraries (default parameters), as well as co-assemblies grouping libraries from the same *S. alterniflora* phenotype and compartment (--mink 40 --maxk 120 --step 20 --min_contig 300) (Peng et al., 2012). The resulting contigs from both individual and co-assemblies were binned using three different algorithms with default options: MaxBin v.2.2.7, MetaBAT v.2.15, and CONCOCT v1.1.0 (Alneberg et al., 2014; Wu et al., 2016; Kang et al.,

591 2019). Recovered bins were dereplicated with DAS Tool v1.1.2 (Sieber et al., 2018), and the output
592 was refined for putative contamination with MAGPurify v2.1.2 (Nayfach et al., 2019).
593 Completeness, contamination, and quality score (Completeness – 5*Contamination) were
594 calculated with MiGA v0.7 (Rodriguez-R et al., 2018a). Recovered MAGs with a quality score
595 less than 50 were considered low quality and discarded. A second round of assembly and binning
596 was performed after discarding short reads that mapped against MAGs. Metagenomic libraries
597 were mapped against MAGs using bowtie2 v2.4.2 with default parameters. Paired reads that
598 mapped against MAGs were discarded using samtools v1.9 (parameters: view -F 2, Li et al., 2009).
599 Filtered metagenomic libraries were co-assembled once again using idba-ud v1.1.3 with pre-error-
600 correction for highly uneven sequencing depth (parameters: --mink 40 --maxk 120 --step 20 --
601 min_contig 300) in four groups: i) tall *S. alterniflora* root, ii) short *S. alterniflora* root, iii) tall *S.*
602 *alterniflora* sediment and rhizosphere, and iv) short *S. alterniflora* sediment and rhizosphere.
603 Binning, MAGs' refinement, and quality control were performed as explained for the first
604 iteration. Finally, MAGs from both iterations were grouped into genomospecies (gspp, singular
605 gsp) by clustering MAGs with ANI > 95% using the MiGA v0.7 derep_wf workflow (Rodriguez-
606 R et al., 2018a). MAGs with the highest quality score were selected as representatives of their gsp,
607 and most downstream analyses were performed with them.

608 Genomospecies relative abundance was estimated for each metagenomic library as in Rodriguez-
609 R et al. (2020). Sequencing depth was calculated per position using bowtie2 v2.4.2 with default
610 parameters (Langmead and Salzberg, 2012), and bedtools genomecov v2.29.2 (parameters: -bga,
611 Quinlan and Hall, 2010). Bedtools output was truncated to keep only the central 80% values, and
612 the mean of all retained positions was calculated using BedGraph.tad.rb from the enveomics
613 collection, a metric defined as TAD_{80} (truncated average sequencing depth) (Rodriguez-R and

614 Konstantinidis, 2016). Relative abundance of each gsp was calculated by dividing TAD_{80} by
615 genome equivalents estimated for each metagenomic library with MicrobeCensus v1.1.0 (Nayfach
616 and Pollard, 2015).

617 4.8 MAGs taxonomy, phylogenetic analysis, and gene functional annotation and expression

618 Taxonomic classification of all MAGs was performed by GTDB-Tk v2.1.0 using the reference
619 database GTDB R07-RS207 (Chaumeil et al., 2022). A maximum likelihood phylogenetic tree of
620 all gspp was constructed using a 400 universal marker genes database in PhyloPhlAn v3.0.58
621 (parameters: -d phylophlan, --msa mafft, --trim trimal, --map_dna diamond, --map_aa diamond, -
622 -tree1 iqtree, --tree2 raxml, --diversity high, --fast, Asnicar et al., 2020). The phylogenetic tree was
623 decorated and visualized in ggtree v2.0.4 (Yu et al., 2018).

624 Protein-encoding genes from all binned MAGs were predicted with Prodigal v2.6.3 using default
625 parameters (Hyatt et al., 2010), and resulting amino acid sequences aligned against the eggNOG
626 database (release 5.0.2) using eggnog-mapper v2.1.9 (Cantalapiedra et al., 2021). The DIAMOND
627 tabular output was filtered by retrieving only the best hit based on bitscore, and removing hits with
628 less than 30% identity and/or less than 50% match length.

629 Metagenomic and metatranscriptomic short reads were mapped against functionally annotated
630 ORFs of all gspp using megablast v2.10.1. Only hits with greater than 95% percent identity and
631 90% read alignment were retained. The roots from the short and tall phenotype had a median of
632 17.4% and 5.4% reads mapping back to the MAGs, respectively. Percent contribution of genes
633 and transcripts to the total microbial community was assessed by dividing the number of hits from
634 each gsp against the total number of functionally annotated short reads (from section 4.7). When
635 assessing the transcript expression profile of a specific gsp, the number of mapped hits per

annotated transcript was normalized by dividing it by gene length (bp) and the median abundance of 10 universal single-copy phylogenetic marker genes of the prokaryotic community (K06942, K01889, K01887, K01875, K01883, K01869, K01873, K01409, K03106, and K03110).

Finally, since the phylogeny of the *dsrAB* gene allows to discriminate between the oxidative and reductive *dsrAB* types, we aligned all recovered genes from our binned gspp to a reference alignment (Müller et al., 2015) with Clustal Omega v1.2.4 (Sievers et al., 2011), and built an approximately-maximum-likelihood phylogenetic tree with FastTree v2.1.11 (Price et al., 2010). Gene type was inferred based on placement in the phylogenetic tree.

4.9 Non binned scaffold analysis

Scaffold-level analysis from all assemblies and co-assemblies was conducted to enhance the representation of short reads mapping back to the nitrogenase and dissimilatory sulfite reductase genes. Prodigal v2.6.3, with default parameters, was used for predicting ORFs (Hyatt et al., 2010). Functional annotation of predicted ORFs was carried out using eggnog-mapper v2.1.9 (database release 5.0.2, --pident 30, --query_cover 50, Cantalapiedra et al., 2021). All ORFs annotated as *dsrA* or *nifK* were clustered at 95% nucleotide identity using cd-hit-est v4.8.1 (Li and Godzik, 2006). Metatranscriptomic short reads were aligned against the representatives from *dsrA* and *nifK* cd-hit-est clusters using megablast, similar to MAGs ORFs (section 4.8). The taxonomy of ORFs not associated with MAGs was classified at the genus level using kaiju v1.10 against the NCBI-nr database (retrieved on May 10th, 2023) (Menzel et al., 2016). In cases where an ORF was not classified by kaiju, the higher taxonomic classification according to eggnog-mapper was used.

4.10 Phylogenetic reconstruction of the *Sedimenticolaceae* family

Publicly available genomes from all species from the *Sedimenticolaceae* family, according to GTDB R07-RS207 and all *Candidatus* Thiodiazotropha genomes from the Osvatic et al. (2023) study, were retrieved from NCBI. A full list and characteristics of genomes used for this analysis is found in Supplementary Data File S10. A phylogenetic tree of all retrieved genomes and binned genomes from this study was constructed in PhyloPhlAn v3.0.58 using 382 out of the PhyloPhlAn 400 universal marker genes database (parameters: -d phylophlan, --msa mafft, --trim trimal, --map_dna diamond, --map_aa diamond, --tree1 fasttree, --tree2 raxml, --diversity low, --accurate, Asnicar et al., 2020). The phylogenetic tree was decorated and visualized using ggtree v2.0.4 (Yu et al., 2018).

4.11 Amplicon analysis of the 16S rRNA

RNA extractions performed for quantification of the 16S rRNA (section 4.4) were reverse transcribed using the SuperScript IV First-Strand Synthesis System kit (Invitrogen) following manufacturer instructions. Amplicon sequencing of the 16S rRNA was performed on cDNA as in Rolando et al. (2022). Amplicons were amplified for the 16S rRNA V4 region using primers 515F (5′- GTGYCAGCMGCCGCGGTAA′) and 806R (5′- GGACTACNVGGGTWTCTAAT′) (Parada et al., 2016; Apprill et al., 2015). Reactions were performed in 5-ng cDNA template in a solution containing DreamTaq buffer, 0.2 mM dNTPs, 0.5 μM of each primer, 1.25 U DreamTaq DNA polymerase, and 0.75 μM of each mitochondrial (mPNA) and plastid (pPNA) peptide nucleic acid (PNA) clamps to reduce plant plastid and mitochondrial cDNA amplification. Amplicons were sequenced on an Illumina MiSeq2000 platform using a 500-cycle v2 sequencing kit (250 paired-end reads) at Georgia Tech Sequencing Core (Atlanta, GA). Cutadapt v3.7 was employed to remove primers from raw fastq files (Martin, 2011). We inferred Amplicon Sequence Variants (ASVs) from quality-filtered reads using DADA2 version 1.10 (Callahan et al., 2016). Chimeric

sequences were removed using the removeBimeraDenovo function in DADA2. Taxonomic assignment was performed utilizing the Ribosomal Database Project (RDP) Naive Bayesian Classifier (Wang et al., 2007) in conjunction with the SILVA SSU rRNA reference alignment (Release 138, Quast et al., 2012). The relative abundance of the *Sedimenticolaceae* and *Desulfosarcinaceae* families, as well as *Ca.* Thiodiazotropha and *Desulfatitalea* genera was estimated by plant compartment and *S. alterniflora* phenotype.

4.12 Analysis of root microbiomes from contrasting ecosystems

Publicly available 16S rRNA gene amplicon datasets, generated from next-generation sequencing, were used to characterize the community assembly of root microbiomes from coastal marine ecosystems. Studies were selected based on google scholar queries using a combination of the following keywords: "salt marsh", "coastal", "wetland", "mangrove", "seagrass", "seabed", "crop", "bog", "plant", "root", "endosphere", "microbial community", "microbiome", “amplicon”, “next-generation sequencing”, “16S rRNA”, and “SSU rRNA”, as well as based on the authors prior knowledge. Only studies that collected environmental samples were included (i.e., no greenhouse or plants grown on potting media were included). When available, paired soil/sediment and rhizosphere samples were also retrieved. Twenty-two studies that met our requirements were selected, collecting a total of 2,911 amplicon samples, with 1,182 of them being from the root compartment across 56 different plant species. Selected plants were categorized into 4 different ecosystem types: seagrass meadows, coastal wetlands, freshwater wetlands, and other terrestrial ecosystems. A complete list of selected amplicon samples with accompanying metadata is available in Supplementary Data File S8.

Cutadapt v3.7 was used to detect and remove primer sequences from all datasets (Martin, 2011). Primer-free sequences were quality filtered using DADA2’s filterAndTrim function [options:

truncLen=c(175,150), maxN=0, maxEE=c(2,2), truncQ=10, rm.phix=TRUE] (Callahan et al., 2016). Trimmed reads were randomly subsampled to a maximum of 20,000 reads using seqtk v.1.3 (Li, 2012) and used as input for dada2 amplicon sequence variant (ASV) calling (Callahan et al., 2016). Chimeras were removed using the removeBimeraDenovo function from the DADA2 package. Taxonomy was assigned to ASVs utilizing the Ribosomal Database Project (RDP) Naive Bayesian Classifier (Wang et al., 2007) against the SILVA SSU rRNA reference alignment [Release 138, (Quast et al., 2012)]. Sequences classified as chloroplast, mitochondrial, and eukaryotic or that did not match any taxonomic phylum were excluded from the dataset. Samples that had less than 5,000 reads were removed at this stage. After all quality filtering steps, we kept on average 13,157 reads from the initial 20,000 subsampled reads per sample (65.8% reads). In order to merge studies from different sequence runs and primer sets, we grouped ASVs at the genus level before merging all studies into a single dataset in phyloseq v1.36 (McMurdie and Holmes, 2013). All selected studies targeted the 16S rRNA gene V3-V4 region, with 55% of them using the 515F/806R primer set.

Microbial community assembly of the root microbiome was analyzed by performing a non-metric multidimensional scaling (NMDS) ordination utilizing the Bray-Curtis dissimilarity distance. Multivariate variation of the Bray-Curtis dissimilarity matrix was partitioned to ecosystem type, and compartment (soil/sediment, rhizosphere, and root), based on a PERMANOVA with 999 permutations performed in vegan v2.5.7 (Oksanen et al., 2013). Finally, putative function for sulfate reduction and sulfur oxidation was assigned based on taxonomic identity at the genus level as in Rolando et al. (2022). Taxa with known sulfate reducing and sulfur oxidizing capability is found in Supplementary Data File S9.

Data availability

The raw metagenomic and metatranscriptomic sequences generated in this study have been deposited in the BioProject database (http://ncbi.nlm.nih.gov/bioproject) under accession codes PRJNA703972 (https://www.ncbi.nlm.nih.gov/bioproject/PRJNA703972/) and PRJNA950121 (https://www.ncbi.nlm.nih.gov/bioproject/PRJNA950121/), respectively. The metagenome-assembled genomes generated in this study have been deposited in the BioProject database under accession code PRJNA703972 (https://www.ncbi.nlm.nih.gov/bioproject/PRJNA703972/). The amplicon 16S rRNA raw reads generated in this study have been deposited in the BioProject database under accession code PRJNA1034039 (https://www.ncbi.nlm.nih.gov/bioproject/PRJNA1034039/). The nitrogen fixation rates generated in this study have been deposited in a Zenodo repository under accession code 7883423 https://doi.org/10.5281/zenodo.7883423 (Kostka Lab, 2023). All accompanying metadata generated in this study are provided in the Supplementary Data Files and the Zenodo repository (Kostka Lab, 2023).

Code availability

Custom scripts used in the present study are publicly available in a Zenodo repository: https://doi.org/10.5281/zenodo.7883423

References:

1. Bulgarelli, D., Schlaeppi, K., Spaepen, S., Van Themaat, E.V.L., Schulze-Lefert, P., 2013. Structure and functions of the bacterial microbiota of plants. Annual review of plant biology, 64:807-838.
2. Trivedi, P., Leach, J.E., Tringe, S.G., Sa, T., Singh, B.K., 2020. Plant–microbiome interactions: from community assembly to plant health. Nature reviews microbiology, 18:607-621.
3. Barbier, E.B., Hacker, S.D., Kennedy, C., Koch, E.W., Stier, A.C. and Silliman, B.R., 2011. The value of estuarine and coastal ecosystem services. Ecological monographs, 81(2), pp.169-193.

4. Duarte, C.M., Losada, I.J., Hendriks, I.E., Mazarrasa, I., Marbà, N., 2013. The role of coastal plant communities for climate change mitigation and adaptation. Nature climate change, 3:961-968.
5. Gandy, E.L., Yoch, D.C., 1988. relationship between nitrogen-fixing sulfate reducers and fermenters in salt marsh sediments and roots of *Spartina alterniflora*. Applied and Environmental Microbiology, 54:2031-2036.
6. Welsh, D.T., Bourgues, S., de Wit, R., Herbert, R.A., 1996. Seasonal variations in nitrogen-fixation (acetylene reduction) and sulphate-reduction rates in the rhizosphere of *Zostera noltii*: nitrogen fixation by sulphate-reducing bacteria. Marine Biology, 125:619-628.
7. Spivak, A.C., Reeve, J., 2015. Rapid cycling of recently fixed carbon in a *Spartina alterniflora* system: a stable isotope tracer experiment. Biogeochemistry, 125:97-114.
8. Thomas, F., Giblin, A.E., Cardon, Z.G., Sievert, S.M., 2014. Rhizosphere heterogeneity shapes abundance and activity of sulfur-oxidizing bacteria in vegetated salt marsh sediments. Frontiers in microbiology, 5:309.
9. Crump, B.C., Wojahn, J.M., Tomas, F., Mueller, R.S., 2018. Metatranscriptomics and amplicon sequencing reveal mutualisms in seagrass microbiomes. Frontiers in microbiology, 9:388.
10. Kolton, M., Rolando, J.L. and Kostka, J.E., 2020. Elucidation of the rhizosphere microbiome linked to Spartina alterniflora phenotype in a salt marsh on Skidaway Island, Georgia, USA. FEMS Microbiology Ecology, 96(4), p.fiaa026.
11. Cúcio, C., Engelen, A.H., Costa, R., Muyzer, G., 2016. Rhizosphere microbiomes of European seagrasses are selected by the plant, but are not species specific. Frontiers in microbiology, 7:440.
12. Rolando, J.L., Kolton, M., Song, T., Kostka, J.E., 2022. The core root microbiome of *Spartina alterniflora* is predominated by sulfur-oxidizing and sulfate-reducing bacteria in Georgia salt marshes, USA. Microbiome, 10:37.
13. Kostka, J.E., Gribsholt, B., Petrie, E., Dalton, D., Skelton, H.,Kristensen, E., 2002. The rates and pathways of carbon oxidation in bioturbated saltmarsh sediments. Limnology and Oceanography, 47:230-240.
14. Jørgensen, B.B., Findlay, A.J., Pellerin, A., 2019. The biogeochemical sulfur cycle of marine sediments. Frontiers in microbiology, 10:849.
15. Capone, D.G., 1982. Nitrogen fixation (acetylene reduction) by rhizosphere sediments of the eelgrass *Zostera marina*. Marine Ecology Progress Series, 10:67-75.
16. McGlathery, K.J., Risgaard-Petersen, N., Christensen, P.B., 1998. Temporal and spatial variation in nitrogen fixation activity in the eelgrass *Zostera marina* rhizosphere. Marine Ecology Progress Series, 168:245-258.
17. Herbert, R.A., 1999. Nitrogen cycling in coastal marine ecosystems. FEMS microbiology reviews, 23:563-590.
18. Nielsen, L.B., Finster, K., Welsh, D.T., Donelly, A., Herbert, R.A., De Wit, R., Lomstein, B.A., 2001. Sulphate reduction and nitrogen fixation rates associated with roots, rhizomes and sediments from *Zostera noltii* and *Spartina maritima* meadows. Environmental Microbiology, 3:63-71.
19. Lamers, L.P., Govers, L.L., Janssen, I.C., Geurts, J.J., Van der Welle, M.E., Van Katwijk, M.M., Van der Heide, T., Roelofs, J.G., Smolders, A.J., 2013. Sulfide as a soil phytotoxin—a review. Frontiers in plant science, 4:268.

20. Mendelssohn, I.A. and Morris, J.T., 2000. Eco-physiological controls on the primary productivity of *Spartina alterniflora*. Concepts and Controversies in Tidal Marsh Ecology, pp.59-80.
21. Martin, B.C., Middleton, J.A., Fraser, M.W., Marshall, I.P., Scholz, V.V., Hausl, B. and Schmidt, H., 2020a. Cutting out the middle clam: lucinid endosymbiotic bacteria are also associated with seagrass roots worldwide. The ISME journal, 14:2901-2905.
22. Petersen, J.M., Kemper, A., Gruber-Vodicka, H., Cardini, U., Van Der Geest, M., Kleiner, M., Bulgheresi, S., Mußmann, M., Herbold, C., Seah, B.K., Antony, C.P., 2016. Chemosynthetic symbionts of marine invertebrate animals are capable of nitrogen fixation. Nature microbiology, 2:16195.
23. König, S., Gros, O., Heiden, S.E., Hinzke, T., Thuermer, A., Poehlein, A., Meyer, S., Vatin, M., Tocny, J., Ponnudurai, R. Daniel, R., 2016. Nitrogen fixation in a chemoautotrophic lucinid symbiosis. Nature microbiology, 2:16193.
24. Osvatic, J.T., Wilkins, L.G., Leibrecht, L., Leray, M., Zauner, S., Polzin, J., Camacho, Y., Gros, O., van Gils, J.A., Eisen, J.A., Petersen, J.M., 2021. Global biogeography of chemosynthetic symbionts reveals both localized and globally distributed symbiont groups. Proceedings of the National Academy of Sciences, 118:e2104378118.
25. Osvatic, J.T., Yuen, B., Kunert, M., Wilkins, L., Hausmann, B., Girguis, P., Lundin, K., Taylor, J., Jospin, G., Petersen, J.M., 2023. Gene loss and symbiont switching during adaptation to the deep sea in a globally distributed symbiosis. The ISME Journal, 17:453-466.
26. Lim, S.J., Alexander, L., Engel, A.S., Paterson, A.T., Anderson, L.C., Campbell, B.J., 2019a. Extensive thioautotrophic gill endosymbiont diversity within a single *Ctena orbiculata* (Bivalvia: Lucinidae) population and implications for defining host-symbiont specificity and species recognition. MSystems, 4:e00280-19.
27. Lim, S.J., Davis, B.G., Gill, D.E., Walton, J., Nachman, E., Engel, A.S., Anderson, L.C., Campbell, B.J., 2019b. Taxonomic and functional heterogeneity of the gill microbiome in a symbiotic coastal mangrove lucinid species. The ISME journal, 13:902-920.
28. Cúcio, C., Overmars, L., Engelen, A.H., Muyzer, G., 2018. Metagenomic analysis shows the presence of bacteria related to free-living forms of sulfur-oxidizing chemolithoautotrophic symbionts in the rhizosphere of the seagrass *Zostera marina*. Frontiers in Marine Science, 5:171.
29. Guimond, J.A., Yu, X., Seyfferth, A.L., Michael, H.A., 2020. Using hydrological-biogeochemical linkages to elucidate carbon dynamics in coastal marshes subject to relative sea level rise. Water Resources Research, 56:e2019WR026302.
30. Donnelly, J.P., Bertness, M.D., 2001. Rapid shoreward encroachment of salt marsh cordgrass in response to accelerated sea-level rise. Proceedings of the National Academy of Sciences, 98:14218-14223.
31. Noyce, G.L., Smith, A.J., Kirwan, M.L., Rich, R.L., Megonigal, J.P., 2023. Oxygen priming induced by elevated CO2 reduces carbon accumulation and methane emissions in coastal wetlands. Nature Geoscience, 16:63-68.
32. Giurgevich, J.R. and Dunn, E.L., 1979. Seasonal patterns of CO_2 and water vapor exchange of the tall and short height forms of *Spartina alterniflora* Loisel in a Georgia salt marsh. Oecologia, 43:139-156.
33. Pezeshki, S.R. and DeLaune, R.D., 1988. Carbon assimilation in contrasting streamside and inland *Spartina alterniflora* salt marsh. Vegetatio:55-61.

34. Chaumeil, P.A., Mussig, A.J., Hugenholtz, P., Parks, D.H., 2022. GTDB-Tk v2: memory friendly classification with the genome taxonomy database. Bioinformatics, 38:5315-5316.
35. Müller, A.L., Kjeldsen, K.U., Rattei, T., Pester, M., Loy, A., 2015. Phylogenetic and environmental diversity of DsrAB-type dissimilatory (bi) sulfite reductases. The ISME journal, 9:1152-1165.
36. Salazar, G., Paoli, L., Alberti, A., Huerta-Cepas, J., Ruscheweyh, H.J., Cuenca, M., Field, C.M., Coelho, L.P., Cruaud, C., Engelen, S., Gregory, A.C., 2019. Gene expression changes and community turnover differentially shape the global ocean metatranscriptome. Cell, 179:1068-1083.
37. Whiting, G.J., Gandy, E.L., Yoch, D.C., 1986. Tight coupling of root-associated nitrogen fixation and plant photosynthesis in the salt marsh grass *Spartina alterniflora* and carbon dioxide enhancement of nitrogenase activity. Applied and environmental microbiology, 52:108-113.
38. Fahimipour, A.K., Kardish, M.R., Lang, J.M., Green, J.L., Eisen, J.A., Stachowicz, J.J., 2017. Global-scale structure of the eelgrass microbiome. Applied and environmental microbiology, 83:e03391-16.
39. Howarth, R.W., 1984. The ecological significance of sulfur in the energy dynamics of salt marsh and coastal marine sediments. Biogeochemistry, 1:5-27.
40. Holmer, M., Gribsholt, B., Kristensen, E., 2002. Effects of sea level rise on growth of *Spartina anglica* and oxygen dynamics in rhizosphere and salt marsh sediments. Marine Ecology Progress Series, 225:197-204.
41. Kristensen, E., Alongi, D.M., 2006. Control by fiddler crabs (*Uca vocans*) and plant roots (*Avicennia marina*) on carbon, iron, and sulfur biogeochemistry in mangrove sediment. Limnology and Oceanography, 51:1557-1571.
42. Koop-Jakobsen, K., Mueller, P., Meier, R.J., Liebsch, G., Jensen, K., 2018. Plant-Sediment Interactions in Salt Marshes–An Optode Imaging Study of O_2, pH, and CO_2 Gradients in the Rhizosphere. Frontiers in plant science, 9:541.
43. Lim, S.J., Davis, B., Gill, D., Swetenburg, J., Anderson, L.C., Engel, A.S., Campbell, B.J., 2021. Gill microbiome structure and function in the chemosymbiotic coastal lucinid *Stewartia floridana*. FEMS Microbiology Ecology, 97(4), p.fiab042.
44. Dincturk, H.B., Demir, V., Aykanat, T., 2011. *Bd* oxidase homologue of photosynthetic purple sulfur bacterium *Allochromatium vinosum* is co-transcribed with a nitrogen fixation related gene. Antonie van Leeuwenhoek, 99:211-220.
45. Borisov, V.B., Siletsky, S.A., Paiardini, A., Hoogewijs, D., Forte, E., Giuffre, A., Poole, R.K., 2021. Bacterial oxidases of the cytochrome *bd* family: Redox enzymes of unique structure, function, and utility as drug targets. Antioxidants & redox signaling, 34(16), pp.1280-1318.
46. Taillefert, M., Neuhuber, S., Bristow, G., 2007. The effect of tidal forcing on biogeochemical processes in intertidal salt marsh sediments. Geochemical Transactions, 8:1-15.
47. Marzocchi, U., Benelli, S., Larsen, M., Bartoli, M. and Glud, R.N., 2019. Spatial heterogeneity and short-term oxygen dynamics in the rhizosphere of *Vallisneria spiralis*: Implications for nutrient cycling. Freshwater Biology, 64:532-543.
48. Petersen, J.M., Yuen, B., 2021. The symbiotic "all-rounders": partnerships between marine animals and chemosynthetic nitrogen-fixing bacteria. Applied and Environmental Microbiology, 87:e02129-20.

49. Morris, J. T., Cahoon, D. R., Callaway, J. C., Craft, C., Neubauer, S. C., Weston, N. B., 2021. Marsh Equilibrium Theory: Implications for Responses to Rising Sea Level. In: FitzGerald, D. M. and Hughes, Z. J. (eds) Salt Marshes: Function, Dynamics, and Stresses. Cambridge: Cambridge University Press, pp. 157–177.
50. Fox-Kemper, B., Hewitt, H.T., Xiao, C., Aðalgeirsdóttir, G., Drijfhout, S.S., et al. 2021. Ocean, cryosphere and sea level change. In Climate Change 2021: The Physical Science Basis. Contribution of Working Group I to the Sixth Assessment Report of the Intergovernmental Panel on Climate Change, ed. V Masson-Delmotte, P Zhai, A Pirani, SL Connors, C Péan, et al., pp. 1211–362. Cambridge, UK: Cambridge Univ. Press
51. Kirwan, M.L., Temmerman, S., Skeehan, E.E., Guntenspergen, G.R., Fagherazzi, S., 2016. Overestimation of marsh vulnerability to sea level rise. Nature Climate Change, 6:253-260.
52. Martin, B.C., Alarcon, M.S., Gleeson, D., Middleton, J.A., Fraser, M.W., Ryan, M.H., Holmer, M., Kendrick, G.A., Kilminster, K., 2020b. Root microbiomes as indicators of seagrass health. FEMS Microbiology Ecology, 96:fiz201.
53. Simmons, T., Caddell, D.F., Deng, S., Coleman-Derr, D., 2018. Exploring the root microbiome: extracting bacterial community data from the soil, rhizosphere, and root endosphere. Journal of visualized experiments: JoVE, 135.
54. Leppänen, S.M., Salemaa, M., Smolander, A., Mäkipää, R., Tiirola, M., 2013. Nitrogen fixation and methanotrophy in forest mosses along a N deposition gradient. Environmental and Experimental Botany, 90:62-69.
55. Lever, M.A., Torti, A., Eickenbusch, P., Michaud, A.B., Šantl-Temkiv, T., Jørgensen, B.B., 2015. A modular method for the extraction of DNA and RNA, and the separation of DNA pools from diverse environmental sample types. Frontiers in Microbiology 6:476.
56. Caporaso, J.G., Lauber, C.L., Walters, W.A., Berg-Lyons, D., Lozupone, C.A., Turnbaugh, P.J., Fierer, N., Knight, R., 2011. Global patterns of 16S rRNA diversity at a depth of millions of sequences per sample. Proceedings of the national academy of sciences, 108:4516-4522.
57. Lundberg, D.S., Yourstone, S., Mieczkowski, P., Jones, C.D., Dangl, J.L., 2013. Practical innovations for high-throughput amplicon sequencing. Nature methods, 10:999-1002.
58. Bushnell, B., 2014. BBTools software package. URL http://sourceforge. net/projects/bbmap.
59. Andrews, S., 2010. FastQC: a quality control tool for high throughput sequence data. Available online at: http://www.bioinformatics.babraham.ac.uk/projects/fastqc/
60. Langmead, B., Salzberg S., 2012. Fast gapped-read alignment with Bowtie 2. Nature Methods, 9:357-359.
61. Li, H., Handsaker, B., Wysoker, A., Fennell, T., Ruan, J., Homer, N., Marth, G., Abecasis, G., Durbin, R., 2009. The sequence alignment/map format and SAMtools. Bioinformatics, 25:2078-2079.
62. Kopylova, E., Noé, L., Touzet, H., 2012. SortMeRNA: fast and accurate filtering of ribosomal RNAs in metatranscriptomic data. Bioinformatics, 28:3211-3217.
63. Johnston, E.R., Kim, M., Hatt, J.K., Phillips, J.R., Yao, Q., Song, Y., Hazen, T.C., Mayes, M.A., Konstantinidis, K.T., 2019. Phosphate addition increases tropical forest soil respiration primarily by deconstraining microbial population growth. Soil Biology and Biochemistry, 130:43-54.

64. Cantalapiedra, C.P., Hernández-Plaza, A., Letunic, I., Bork, P., Huerta-Cepas, J., 2021. eggNOG-mapper v2: functional annotation, orthology assignments, and domain prediction at the metagenomic scale. Molecular biology and evolution, 38:5825-5829.
65. Oksanen, J., Blanchet, F.G., Friendly, M., Kindt, R., Legendre, P., McGlinn, D., Minchin, P.R., O'Hara, R.B., Simpson, G.L., Solymos, P., Stevens, M.H.H., Szoecs, E., Wagner, H., 2020. vegan: Community Ecology Package. R package version 2.5-7. https://CRAN.R-project.org/package=vegan
66. Rodriguez-R, L. M., Gunturu, S., Tiedje, J. M., Cole, J. R., Konstantinidis, K. T., 2018b. Nonpareil 3: fast estimation of metagenomic coverage and sequence diversity. MSystems, 3:e00039-18.
67. Rodriguez-R, L.M., Tsementzi, D., Luo, C., Konstantinidis, K.T., 2020. Iterative subtractive binning of freshwater chronoseries metagenomes identifies over 400 novel species and their ecologic preferences. Environmental Microbiology, 22:3394-3412.
68. Peng, Y., Leung, H.C., Yiu, S.M., Chin, F.Y., 2012. IDBA-UD: a de novo assembler for single-cell and metagenomic sequencing data with highly uneven depth. Bioinformatics, 28:1420-1428.
69. Alneberg, J., Bjarnason, B.S., De Bruijn, I., Schirmer, M., Quick, J., Ijaz, U.Z., Lahti, L., Loman, N.J., Andersson, A.F. and Quince, C., 2014. Binning metagenomic contigs by coverage and composition. Nature methods, 11(11), pp.1144-1146.
70. Wu, Y.W., Simmons, B.A., Singer, S.W., 2016. MaxBin 2.0: an automated binning algorithm to recover genomes from multiple metagenomic datasets. Bioinformatics, 32:605-607.
71. Kang, D.D., Li, F., Kirton, E., Thomas, A., Egan, R., An, H. and Wang, Z., 2019. MetaBAT 2: an adaptive binning algorithm for robust and efficient genome reconstruction from metagenome assemblies. PeerJ, 7, p.e7359.
72. Sieber, C.M., Probst, A.J., Sharrar, A., Thomas, B.C., Hess, M., Tringe, S.G., Banfield, J.F., 2018. Recovery of genomes from metagenomes via a dereplication, aggregation and scoring strategy. Nature microbiology, 3:836-843.
73. Nayfach, S., Shi, Z.J., Seshadri, R., Pollard, K.S. and Kyrpides, N.C., 2019. insights from uncultivated genomes of the global human gut microbiome. Nature, 568:505-510.
74. Rodriguez-R, L.M., Gunturu, S., Harvey, W.T., Rosselló-Mora, R., Tiedje, J.M., Cole, J.R., Konstantinidis, K.T., 2018a. The Microbial Genomes Atlas (MiGA) webserver: taxonomic and gene diversity analysis of Archaea and Bacteria at the whole genome level. Nucleic acids research, 46:W282-W288.
75. Quinlan, A.R., Hall, I.M., 2010. BEDTools: a flexible suite of utilities for comparing genomic features. Bioinformatics, 26:841-842.
76. Rodriguez-R, L.M., Konstantinidis, K.T., 2016. The enveomics collection: a toolbox for specialized analyses of microbial genomes and metagenomes. PeerJ Prepr 4: e1900v1.
77. Nayfach, S., Pollard, K.S. 2015. Average genome size estimation improves comparative metagenomics and sheds light on the functional ecology of the human microbiome. Genome Biology, 16:51.
78. Yu, G., Lam, T.T.Y., Zhu, H., Guan, Y., 2018. Two methods for mapping and visualizing associated data on phylogeny using ggtree. Molecular biology and evolution, 35:3041-3043.

79. Hyatt, D., Chen, G.L., LoCascio, P.F., Land, M.L., Larimer, F.W. and Hauser, L.J., 2010. Prodigal: prokaryotic gene recognition and translation initiation site identification. BMC bioinformatics, 11(1), p.119.
80. Sievers, F., Wilm, A., Dineen, D., Gibson, T.J., Karplus, K., Li, W., Lopez, R., McWilliam, H., Remmert, M., Söding, J., Thompson, J.D., 2011. Fast, scalable generation of high-quality protein multiple sequence alignments using Clustal Omega. Molecular systems biology, 7:539.
81. Price, M.N., Dehal, P.S. and Arkin, A.P., 2010. FastTree 2–approximately maximum-likelihood trees for large alignments. PloS one, 5:e9490.
82. Li, W., Godzik, A., 2006. Cd-hit: a fast program for clustering and comparing large sets of protein or nucleotide sequences. Bioinformatics, 22:1658-1659.
83. Menzel, P., Ng, K.L., Krogh, A., 2016. Fast and sensitive taxonomic classification for metagenomics with Kaiju. Nature communications, 7:11257.
84. Asnicar, F., Thomas, A.M., Beghini, F., Mengoni, C., Manara, S., Manghi, P., Zhu, Q., Bolzan, M., Cumbo, F., May, U., Sanders, J.G., 2020. Precise phylogenetic analysis of microbial isolates and genomes from metagenomes using PhyloPhlAn 3.0. Nature communications, 11:1-10.
85. Parada, A.E., Needham, D.M., Fuhrman, J.A., 2016. Every base matters: assessing small subunit rRNA primers for marine microbiomes with mock communities, time series and global field samples. Environmental microbiology, 18:1403-1414.
86. Apprill, A., McNally, S., Parsons, R. and Weber, L., 2015. Minor revision to V4 region SSU rRNA 806R gene primer greatly increases detection of SAR11 bacterioplankton. Aquatic Microbial Ecology, 75:129-137.
87. Martin, M., 2011. Cutadapt removes adapter sequences from high-throughput sequencing reads. EMBnet. journal, 17:10-12.
88. Callahan, B.J., McMurdie, P.J., Rosen, M.J., Han, A.W., Johnson, A.J.A., Holmes, S.P., 2016. DADA2: High-resolution sample inference from Illumina amplicon data. Nature methods, 13:581-583.
89. Wang, Q., Garrity, G.M., Tiedje, J.M., Cole, J.R., 2007. Naive Bayesian classifier for rapid assignment of rRNA sequences into the bacterial taxonomy. Applied and environmental microbiology, 73:5261-5267.
90. Quast, C., Pruesse, E., Yilmaz, P., Gerken, J., Schweer, T., Yarza, P., Peplies, J., Glöckner, F.O., 2012. The SILVA ribosomal RNA gene database project: improved data processing and web-based tools. Nucleic acids research, 41:D590-D596.
91. Li, H., 2012. seqtk Toolkit for processing sequences in FASTA/Q formats. GitHub.
92. McMurdie, P.J. and Holmes, S., 2013. phyloseq: an R package for reproducible interactive analysis and graphics of microbiome census data. PloS one, 8:e61217.
93. Kostka Lab. (2023). kostka-lab/Spartina_root_diazotrophy: Data associated with diazotrophic symbionts of *Spartina alterniflora* (Spartina). Zenodo. https://doi.org/10.5281/zenodo.7883423

Acknowledgements

This work was supported in part by an institutional grant (NA18OAR4170084) to the Georgia Sea Grant College Program from the National Sea Grant Office, National Oceanic and Atmospheric

Administration, US Department of Commerce, and by a grant from the National Science Foundation (DEB 1754756). Any opinions, findings, and conclusions or recommendations expressed in this material are those of the authors and do not necessarily reflect the views of the National Science Foundation.

Author information

Contributions

Conceptualization: J.L.R., M.K., J.T.M., and J.E.K. Field sampling and analysis: J.L.R., M.K., T.S., Y.L., and J.E.K. Bioinformatic analysis: J.L.R., M.K., P.P., R.C., and K.T.K. Funding acquisition: J.E.K. Writing—original draft: J.L.R. with inputs from all authors.

Corresponding author

Correspondence to Joel E. Kostka

Competing Interests Statement

The authors declare no competing interests.

Figure Legends

Figure 1. *Spartina alterniflora* biomass gradient as a natural laboratory. A gradient in *S. alterniflora* aboveground biomass is commonly observed with tall plants growing at the levees next to large tidal creeks and a short phenotype of *S. alterniflora* dominating the interior of the marsh. Sediments from the tall *S. alterniflora* zone are characterized as a more oxidized environment with higher levels of iron, coupled nitrification-denitrification as well as higher rates of organic matter hydrolysis and mineralization. Conversely, sediments from the short phenotype tend to be more chemically reduced, with higher rates of sulfate reduction, elevated porewater salinity, and less bioturbation and tidal flushing. Roots from the short *S. alterniflora* phenotype have been proposed to harbor sulfur-oxidizing bacteria (SOB) that benefit the plant by detoxifying the root environment.

Figure 2. Prokaryotic abundance, functional diversity, and activity are determined by *Spartina alterniflora* phenotype and microbiome compartment. Metagenomic nonpareil diversity, 16S rRNA gene and transcript abundance as quantified by qPCR and RT-qPCR, respectively (n = 4 per compartment and *S. alterniflora* phenotype) (a). Principal coordinate analysis (PCoA) ordination plot based on the Bray-Curtis dissimilatory index of functional profiles from KEGG orthology annotations (KO level) of metagenome and metatranscriptome libraries (b). In boxplots, boxes are defined by the upper and lower interquartile; the median is represented as a horizontal line within the boxes; whiskers extend to the most extreme data point which is no more than 1.5 times the interquartile range. Different letter indicates statistical difference based on pairwise Mann-Whitney tests (two-sided, p-value < 0.05).

Figure 3. Phylogenetic reconstruction of 160 dereplicated metagenome assembled genomes (MAGs, > 50 quality-score) binned from *Spartina alterniflora* sediment, rhizosphere, and root samples. Outer rim shows the presence/absence of genes for carbon fixation (*RuBisCO*), nitrogen fixation (*nifHDK*), thiosulfate oxidation (*soxABXYZ*), dissimilatory sulfite reduction/oxidation (*dsrAB*), nitrification (*amoCAB*), denitrification, and dissimilatory nitrate reduction to ammonium (DNRA). *Desulfosarcinaceae* and *Candidatus* Thiodiazotropha genomospecies are highlighted within pink and orange polygons, respectively.

Figure 4. Drivers and metagenome assembled genomes (MAGs) associated with rates of N fixation in the salt marsh environment. Rates of N fixation (under anoxic and oxic conditions) and ^{15}N isotopic natural abundance per microbiome compartment and *Spartina alterniflora* phenotype (n = 4 per compartment and *S. alterniflora* phenotype) (a). ^{15}N natural abundance was expressed as the per mille (‰) deviation from air ^{15}N:^{14}N ratio ($\delta^{15}N$). Normalized transcript relative abundance of the nitrogenase gene (*nifK*), and the reductive and oxidative *dsrA* types per microbiome compartment and *S. alterniflora* phenotype (b). Percentage contribution of nitrogenase (*nifK*), reductive, and oxidative types of *dsrA* short read transcripts mapping to the most active MAGs and open reading frames (ORFs) obtained from unbinned scaffolds (c). In boxplots, boxes are defined by the upper and lower interquartile; the median is represented as a horizontal line within the boxes; whiskers extend to the most extreme data point which is no more than 1.5 times the interquartile range. Statistical significance based on non-parametric pairwise Mann-Whitney tests (two-sided). n.s. = p-value > 0.05, * p-value < 0.05, ** p-value < 0.01.

Figure 5. Phylogenetic tree of the *Sedimenticolaceae* family. Taxonomic annotation of the *Candidatus* Thiodiazotropha genus was based on Osvatic et al. (2023). The diagram next to the species name recognizes genomes recovered as symbionts of eukaryotic organisms. The average relative abundance of the metagenome assembled genomes (MAGs) from the present study is shown in the adjacent panels per microbiome compartment and *Spartina alterniflora* phenotype. Relative abundance was calculated at the DNA-level based on average coverage per position in

metagenomic libraries. Purple sulfur bacteria *Allochromatium vinosum* was used as an outgroup for the phylogenetic tree.

Figure 6: Roots from marine influenced ecosystems assemble a distinct microbial community enriched by bacteria known to conserve energy from sulfur metabolism. Non-metric multidimensional scaling (NMDS) ordination plot based on the Bray-Curtis dissimilatory index of root-associated prokaryotic communities at the genus level, colored by ecosystem type (a). Relative abundance of putative sulfur-oxidizing (b) and sulfate-reducing root bacteria (c) by ecosystem type. Prokaryotic communities were characterized by analyzing an SSU rRNA gene amplicon dataset of 1,182 samples assessing roots from 56 plant species. In boxplots, boxes are defined by the upper and lower interquartile; the median is represented as a horizontal line within the boxes; whiskers extend to the most extreme data point which is no more than 1.5 times the interquartile range. Different letter indicates statistical difference based on pairwise Mann-Whitney tests (two-sided, p-value < 0.05). NMDS stress: 0.10.

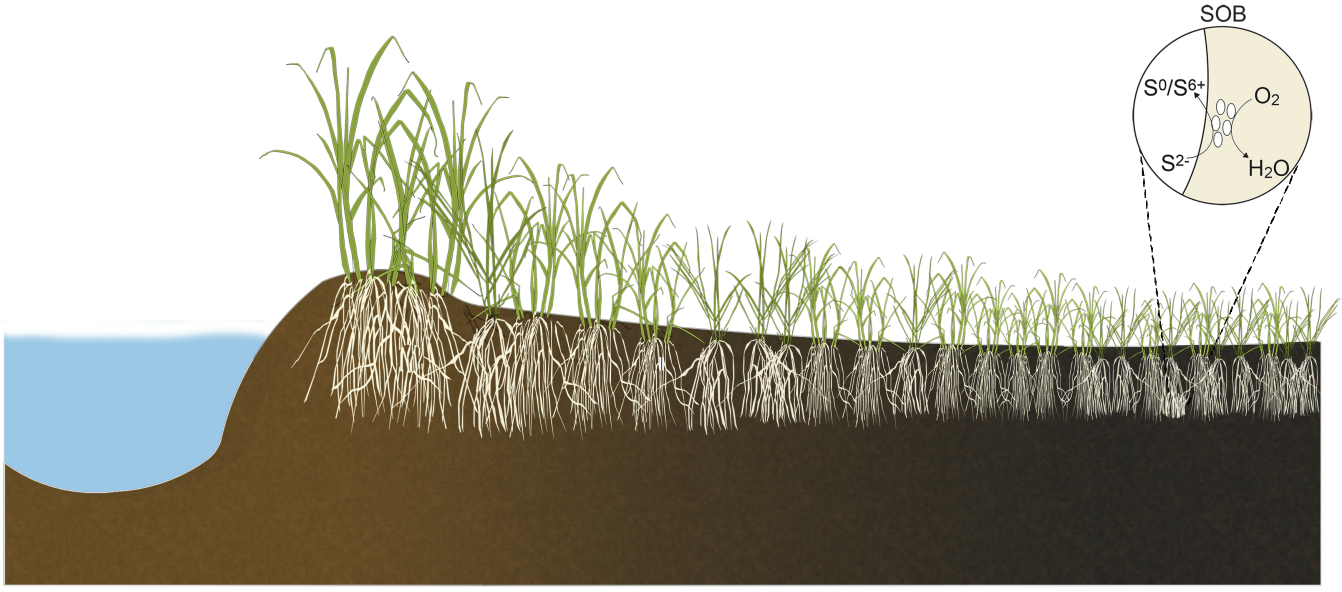

- ↑ Interstitial [Fe^{2+}]
- ↑ Rates of Fe^{3+} reduction
- ↑ Bioturbation and tidal flushing
- ↑ Rates of coupled nitrification-denitrification
- ↑ Rates of SOM hydrolysis and mineralization

- ↑ Interstitial [HS^-]
- ↑ Porewater salinity
- ↑ Rates of SO_4^{2+} reduction

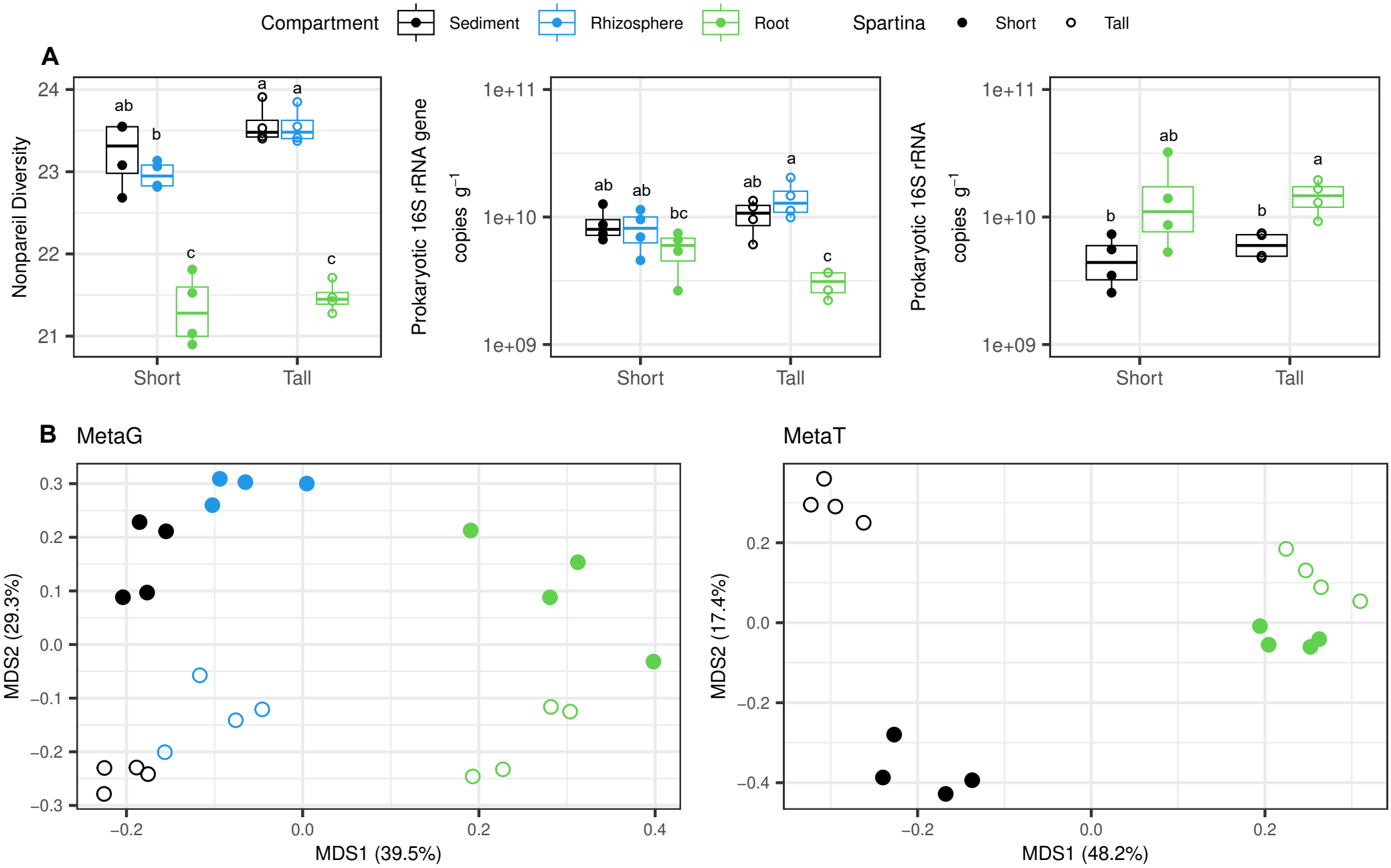
Compartment
Sediment
Rhizosphere
Root
Spartina
Short
Tall
A
Nonpareil Diversity
Prokaryotic 16S rRNA gene copies g−1
Prokaryotic 16S rRNA copies g−1
Short
Tall
B
MetaG
MetaT
MDS2 (29.3%)
MDS1 (39.5%)
MDS2 (17.4%)
MDS1 (48.2%)

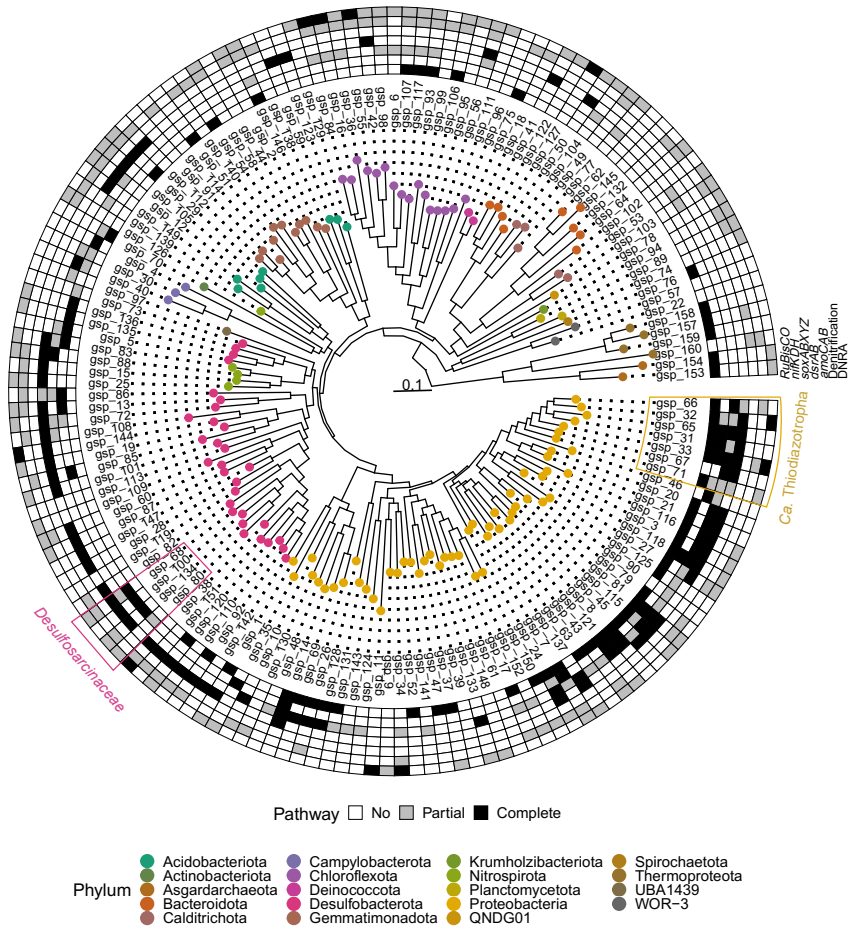
0.1
RuBisCO
nirK/D/X/Y/Z
sqrAB
amoCAB
Nitrification
DNRA
Ca. Thiodiazotropha
Desulfosarcinaceae
Pathway
No
Partial
Complete
Phylum
Acidobacteriota
Actinobacteriota
Asgardarchaeota
Bacteroidota
Calditrichota
Campylobacterota
Chloroflexota
Deinococcota
Desulfobacterota
Gemmatimonadota
Krumholzibacteriota
Nitrospirota
Planctomycetota
Proteobacteria
QNDG01
Spirochaetota
Thermoproteota
UBA1439
WOR-3

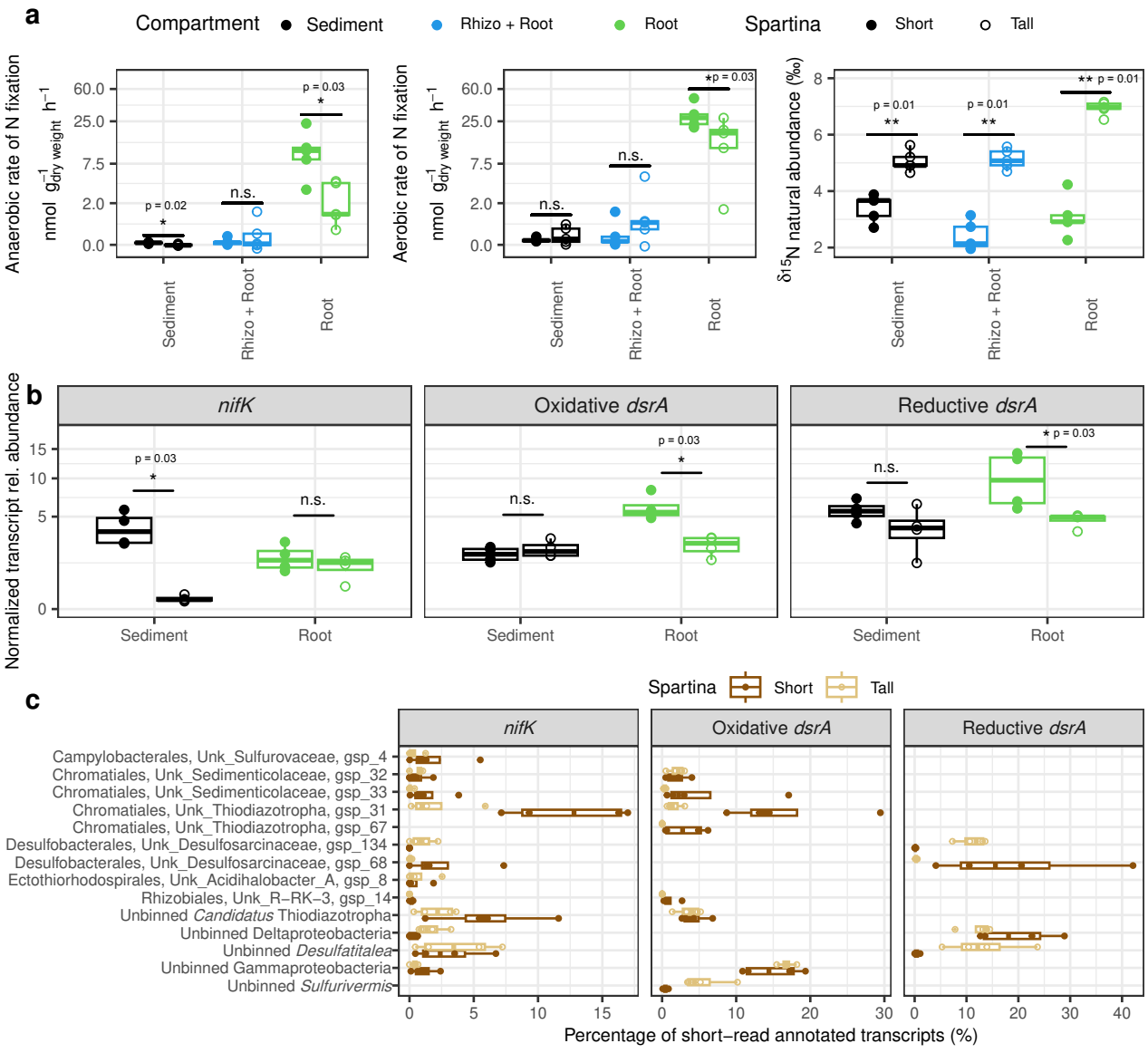
a
Compartment
Sediment
Rhizo + Root
Root
Spartina
Short
Tall
Anaerobic rate of N fixation
nmol $g^{-1}_{dry\ weight}$ h^{-1}
Aerobic rate of N fixation
nmol $g^{-1}_{dry\ weight}$ h^{-1}
$\delta^{15}N$ natural abundance (‰)
p = 0.02
p = 0.03
p = 0.01
n.s.
Sediment
Rhizo + Root
Root
b
Normalized transcript rel. abundance
nifK
Oxidative dsrA
Reductive dsrA
c
Spartina
Short
Tall
Campylobacterales, Unk_Sulfurovaceae, gsp_4
Chromatiales, Unk_Sedimenticolaceae, gsp_32
Chromatiales, Unk_Sedimenticolaceae, gsp_33
Chromatiales, Unk_Thiodiazotropha, gsp_31
Chromatiales, Unk_Thiodiazotropha, gsp_67
Desulfobacterales, Unk_Desulfosarcinaceae, gsp_134
Desulfobacterales, Unk_Desulfosarcinaceae, gsp_68
Ectothiorhodospirales, Unk_Acidihalobacter_A, gsp_8
Rhizobiales, Unk_R−RK−3, gsp_14
Unbinned Candidatus Thiodiazotropha
Unbinned Deltaproteobacteria
Unbinned Desulfatitalea
Unbinned Gammaproteobacteria
Unbinned Sulfurivermis
Percentage of short−read annotated transcripts (%)

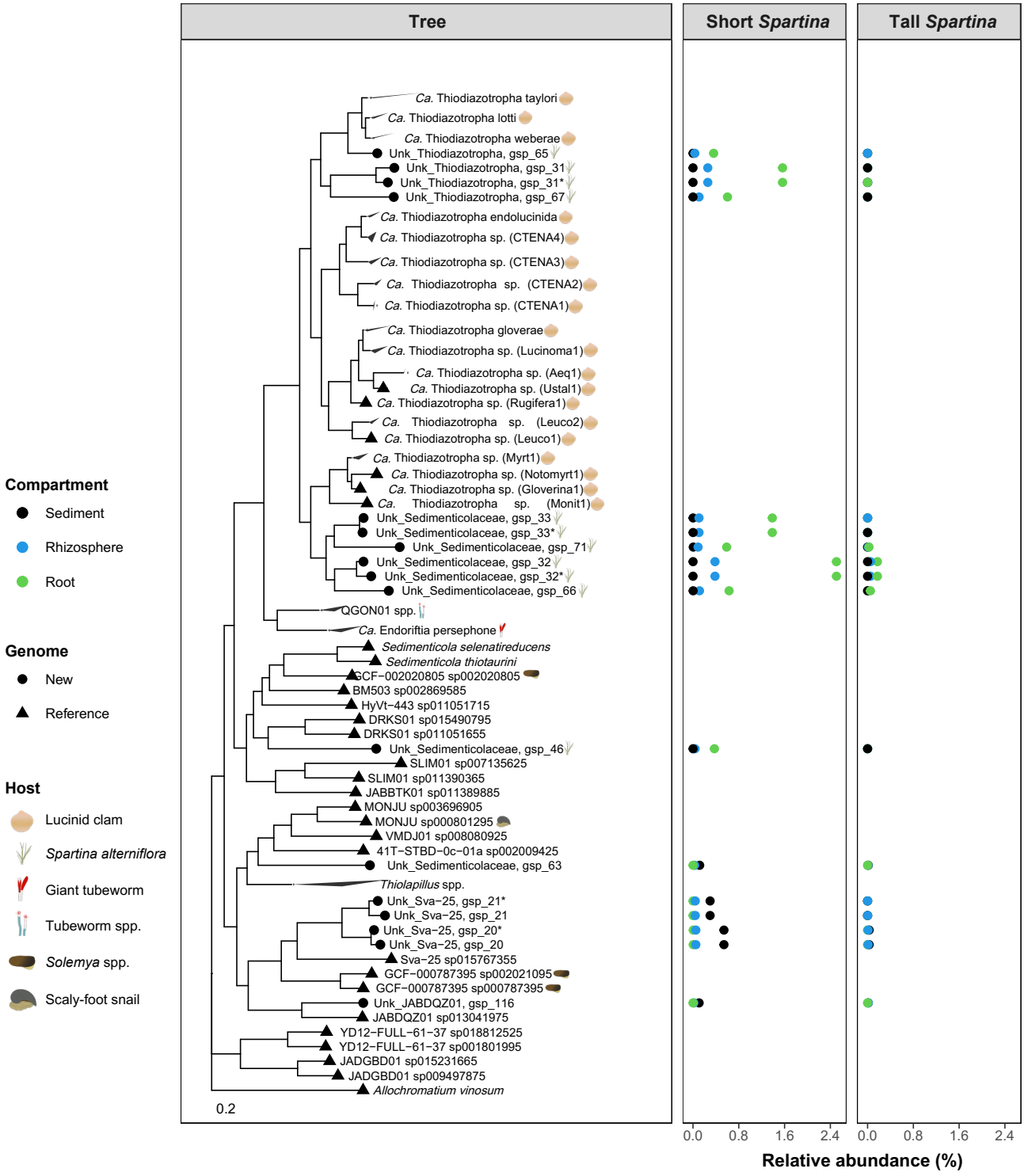
Tree
Short Spartina
Tall Spartina
Ca. Thiodiazotropha taylori
Ca. Thiodiazotropha lotti
Ca. Thiodiazotropha weberae
Unk_Thiodiazotropha, gsp_65
Unk_Thiodiazotropha, gsp_31
Unk_Thiodiazotropha, gsp_31*
Unk_Thiodiazotropha, gsp_67
Ca. Thiodiazotropha endolucinida
Ca. Thiodiazotropha sp. (CTENA4)
Ca. Thiodiazotropha sp. (CTENA3)
Ca. Thiodiazotropha sp. (CTENA2)
Ca. Thiodiazotropha sp. (CTENA1)
Ca. Thiodiazotropha gloverae
Ca. Thiodiazotropha sp. (Lucinoma1)
Ca. Thiodiazotropha sp. (Aeq1)
Ca. Thiodiazotropha sp. (Ustal1)
Ca. Thiodiazotropha sp. (Rugifera1)
Ca. Thiodiazotropha sp. (Leuco2)
Ca. Thiodiazotropha sp. (Leuco1)
Ca. Thiodiazotropha sp. (Myrt1)
Ca. Thiodiazotropha sp. (Notomyrt1)
Ca. Thiodiazotropha sp. (Gloverina1)
Ca. Thiodiazotropha sp. (Monit1)
Unk_Sedimenticolaceae, gsp_33
Unk_Sedimenticolaceae, gsp_33*
Unk_Sedimenticolaceae, gsp_71
Unk_Sedimenticolaceae, gsp_32
Unk_Sedimenticolaceae, gsp_32*
Unk_Sedimenticolaceae, gsp_66
QGON01 spp.
Ca. Endoriftia persephone
Sedimenticola selenatireducens
Sedimenticola thiotaurini
GCF−002020805 sp002020805
BM503 sp002869585
HyVt−443 sp011051715
DRKS01 sp015490795
DRKS01 sp011051655
Unk_Sedimenticolaceae, gsp_46
SLIM01 sp007135625
SLIM01 sp011390365
JABBTK01 sp011389885
MONJU sp003696905
MONJU sp000801295
VMDJ01 sp008080925
41T−STBD−0c−01a sp002009425
Unk_Sedimenticolaceae, gsp_63
Thiolapillus spp.
Unk_Sva−25, gsp_21*
Unk_Sva−25, gsp_21
Unk_Sva−25, gsp_20*
Unk_Sva−25, gsp_20
Sva−25 sp015767355
GCF−000787395 sp002021095
GCF−000787395 sp000787395
Unk_JABDQZ01, gsp_116
JABDQZ01 sp013041975
YD12−FULL−61−37 sp018812525
YD12−FULL−61−37 sp001801995
JADGBD01 sp015231665
JADGBD01 sp009497875
Allochromatium vinosum
0.2
0.0
0.8
1.6
2.4
0.0
0.8
1.6
2.4
Relative abundance (%)
Compartment
Sediment
Rhizosphere
Root
Genome
New
Reference
Host
Lucinid clam
Spartina alterniflora
Giant tubeworm
Tubeworm spp.
Solemya spp.
Scaly-foot snail

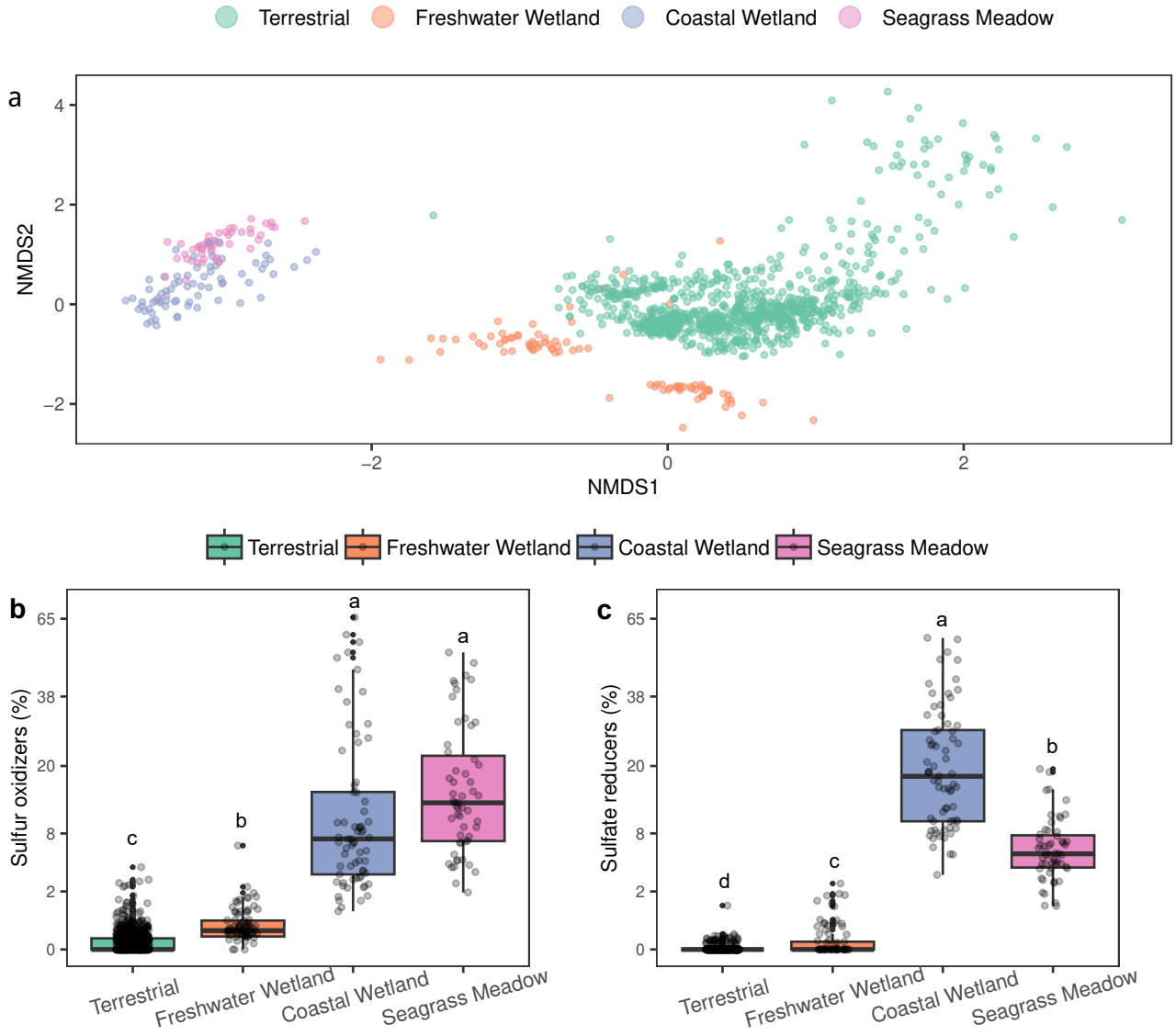
Terrestrial
Freshwater Wetland
Coastal Wetland
Seagrass Meadow
a
NMDS2
NMDS1
b
Sulfur oxidizers (%)
c
a
a
b
Terrestrial
Freshwater Wetland
Coastal Wetland
Seagrass Meadow
c
Sulfate reducers (%)
d
c
a
b